Geomorphology 374 (2021) 107512

Contents lists available at ScienceDirect

Geomorphology

journal homepage: www.elsevier.com/locate/geomorph

Drainage integration of the Salt and Verde rivers in a Basin and Range extensional landscape, central Arizona, USA

Steve J. Skotnicki [a], Yeong B. Seong [b], Ronald I. Dorn [c,*], Phillip H. Larson [d], Jersy DePonty [e], Ara Jeong [f]

[a] 281 W. Amoroso Dr, Gilbert, AZ 85233, USA
[b] Department of Geography Education, Korea University, Seoul 136-701, Republic of Korea
[c] School of Geographical Sciences & Urban Planning, Arizona State University, Tempe, AZ 85287, USA
[d] EARTH Systems Laboratory, Earth Science Programs, Department of Geography, Minnesota State University-Mankato, Mankato, MN 56001-6026, USA
[e] Groundwater Resources and Geohydrology, Salt River Project, 1521 N. Project Dr., Tempe, AZ 85281-1206, USA
[f] Department of Geography Education, Korea University, Seoul 136-701, Republic of Korea

ARTICLE INFO

Article history:
Received 14 July 2019
Received in revised form 11 November 2020
Accepted 11 November 2020
Available online 14 November 2020

Keywords:
Aggradation
Lake overflow
Piracy
Overfill
Transverse stream

ABSTRACT

The Salt River and Verde River watersheds provide downstream metropolitan Phoenix, Arizona, USA with much of its water supply, and this paper explains how these rivers integrated in an extensional tectonic setting. Near the end of the Pliocene, segments of the proto-Salt and proto-Verde watersheds of central Arizona consisted of local drainage networks supplying water and sediment into internally drained basins, including depressions occupied by late Pliocene natural lakes occupying the Verde Valley and Tonto basins. A key location, the lower Verde River valley (LVRV), is where the modern-day drainages of the Salt and Verde now meet downstream of these Pliocene lakes. At the time of the Nomlaki tuff deposition ~3.3 Ma, a condition of sediment overfill existed in the LVRV, although there was no exoreic drainage and a playa was still maintained. A fanglomerate unit, named here the Rolls formation, spilled over a bedrock sill and an alluvial-fan ramp transported sediment into the Higley Basin that underlies the eastern part of metropolitan Phoenix. Lithologies of preserved remnants of this Pliocene alluvial-fan system match well cuttings of buried sediment in the Higley Basin with a cosmogenic burial isochron age of 3.90 ± 0.70 Ma. Based on cosmogenic burial isochron ages, ancestral Salt River gravels started depositing on top of this fan ramp between 2.8 and 2.2 Ma. Deposition of Salt and Verde river gravels in the Higley Basin continued for ~2 million years and eventually led to an aggradational piracy event that overtopped a bedrock ridge immediately east of Phoenix's Sky Harbor Airport. A cosmogenic burial age of 460 ± 23 ka is a rough maximum age for this river avulsion that relocated the Salt River into the Luke Basin that underlies western metropolitan Phoenix. Available chronometric data are not precise enough to determine whether the Salt River or Gila River integrated first. All of the exoreic rivers of western North America's Basin and Range Province — the lower Colorado, Gila, Rio Grande, Salt, and Verde rivers — employed lake overflow to integrate across half-graben, graben, rift and supradetachment tectonic settings.

1. Introduction

Extensional tectonics influence the development of relief and thereby impact geomorphic processes and associated landforms (Withjack et al., 2002; Burchfiel et al., 2008). Concomitantly, different styles of extensional tectonics can constrain how geomorphic systems develop within an extensional landscape (Friedmann and Burbank, 1995). In central and southern Arizona, USA, the Basin and Range Province (BRP) hosts a variety of landscapes resulting from different extensional tectonic processes, including the lower Colorado rift through which the Colorado River flows and supradetachment with metamorphic core complexes as well as grabens and half-grabens exemplified in the Phoenix metropolitan area (Reynolds, 1985; Spencer and Reynolds, 1989; Reynolds and Lister, 1990; Livaccari et al., 1995).

Recent research in the BRP reveals a revitalization of interest in the development and evolution of fluvial systems. Much of this rejuvenation focuses on understanding the processes that result in through-flowing, transverse drainage networks (Meek, 1989; Meek, 2004; House et al., 2008; Douglass et al., 2009a; Larson et al., 2010; Roskowski et al., 2010; Spencer et al., 2013; Jungers and Heimsath, 2016; Gootee et al., 2020; Meek, 2020; Youberg et al., 2020). As this cumulative body of work has progressed, research on the Rio Grande (Connell et al., 2005; Repasch et al., 2017) and lower Colorado (House et al., 2008; Pearthree and House, 2014; Howard et al., 2015) similarly support a general drainage integration model in the BRP proposed by Meek (1989, 2004, 2020). In this

* Corresponding author.
E-mail addresses: sjskotnicki@gmail.com (S.J. Skotnicki), ybseong@korea.ac.kr (Y.B. Seong), ronald.dorn@asu.edu (R.I. Dorn), phillip.larson@mnsu.edu (P.H. Larson), Jersy.DePonty@srpnet.com (J. DePonty), ara0408@korea.ac.kr (A. Jeong).

https://doi.org/10.1016/j.geomorph.2020.107512
0169-555X/

conceptual model, river systems overcome topographic and structural impediments to flow, becoming transverse drainages, through a combination of sediment infilling of structural basins and lake overflow (cf. Davis, 1933; Hilgendorft et al., 2020).

The course of the modern-day Salt River of central Arizona (Fig. 1) had no structural precursor (e.g., a rift) to aid in river integration. Instead, the Salt River crossed structural barriers to flow like the Tonto Basin and lower Verde River valley (LVRV) half-grabens, as well as the supradetachment Higley and Luke basins that underlie the eastern and western halves of metropolitan Phoenix, respectively (Fig. 2). Therefore, the Salt and Verde rivers represent an opportunity to develop a better understanding of how through-flowing drainages integrate across a variety of extensional tectonic settings. Therefore, this manuscript presents a synthesis of new and prior data to construct the pre-integration landscape and hypothesize a sequence of processes and a chronology of integration that resulted in a through-flowing Salt and Verde river system traversing Arizona, USA.

1.1. Overview of the Salt and Verde rivers of central Arizona

The BRP of western North America contains mostly endorheic drainage basins from extensional tectonic processes. With the exception of the Colorado (Blackwelder, 1934; Pearthree and House, 2014) and Rio Grande (Connell et al., 2005) rivers, much of the BRP lacks through-flowing river networks. Arizona's portion of the BRP is unique in that it contains three large rivers with discharges that would reach the ocean naturally: the Gila River and its large tributaries of the Salt and Verde rivers (Fig. 1).

The Salt and Verde watersheds originate in the elevated mountainous terrain near the edge of the Colorado Plateau of central Arizona. Here, they cross several structural basins and converge in a formerly closed endorheic basin just before discharge abruptly exits into the broad, flat Salt River valley on the eastern margin of the BRP (Figs. 1 and 2). The combined discharge of the Salt and Verde perennial waters allowed the Huhugam civilization to flourish until about 600 yr ago (Bostwick, 2002). Subsequent colonization by Europeans in what is now metropolitan Phoenix also depended on this stable water supply.

Within the last eighty years, advancements in technology allowed the drilling of thousands of wells to take advantage of abundant groundwater. Like other arid regions, where evapotranspiration rates far exceed precipitation, surface water and groundwater aquifers are vital to the existence of cities within these environments. In the case of metropolitan Phoenix, surface and groundwater resources owe their existence to the Salt and Verde systems (Laney and Hahn, 1986; Skotnicki and DePonty, 2020) and geomorphic processes that integrated former endorheic basins and resulting in the modern rivers and their sedimentary deposits. Understanding the origin and evolution of the Salt and Verde system requires assessing the processes that result in transverse drainages. The Salt and Verde contain multiple examples, along the modern course of both rivers, of crossing topographic and structural features that should seemingly represent a barrier to flow. Prior modeling and literature synthesis details four mechanisms that can result in transverse drainages and also provides criteria to determine the integrating process: antecedence, superimposition, piracy, or lake overflow (Douglass and Schmeeckle, 2007; Douglass et al., 2009a; Douglass et al., 2009b).

The Salt and Verde rivers cannot be antecedent, because they did not exist prior to the development of Basin and Range topography (Eaton, 1982; Faulds, 1986; Spencer et al., 2001). The earliest evidence of a through-flowing Salt River is found in well logs of sediments within

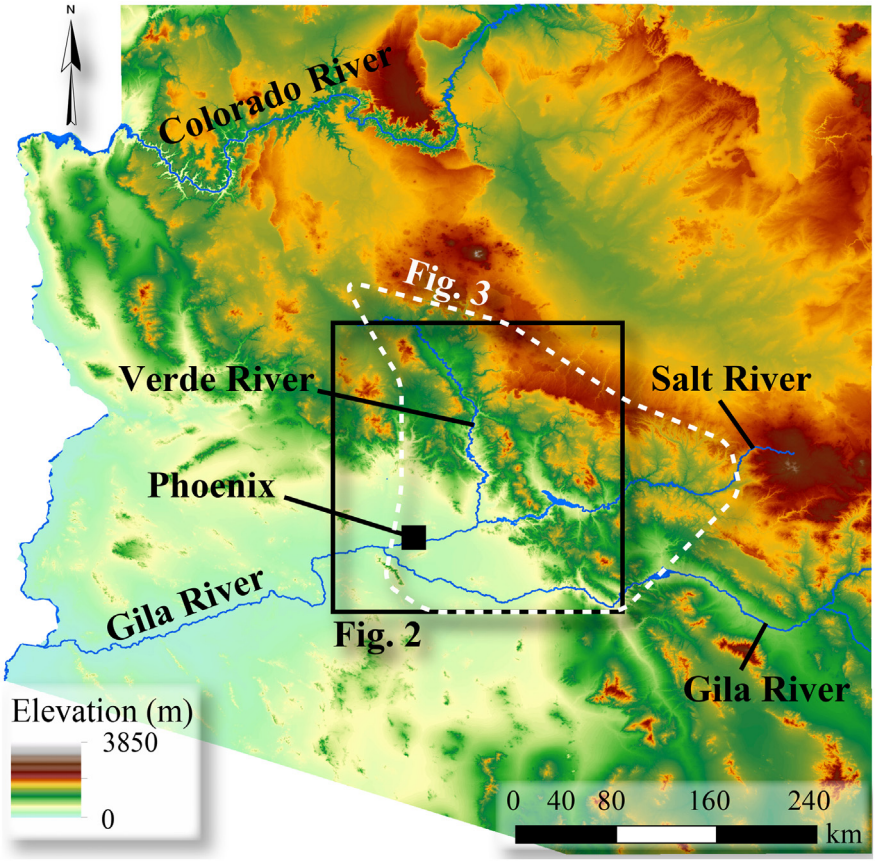

Fig. 1. Arizona topography, highlighting the exoreic Colorado, Gila, Verde, Salt and Rio Grande rivers that integrated across the lowlands of the extensional tectonic terrain of the Basin and Range Province. The polygons identify the framing of Fig. 2 and the modern scene in Fig. 3.

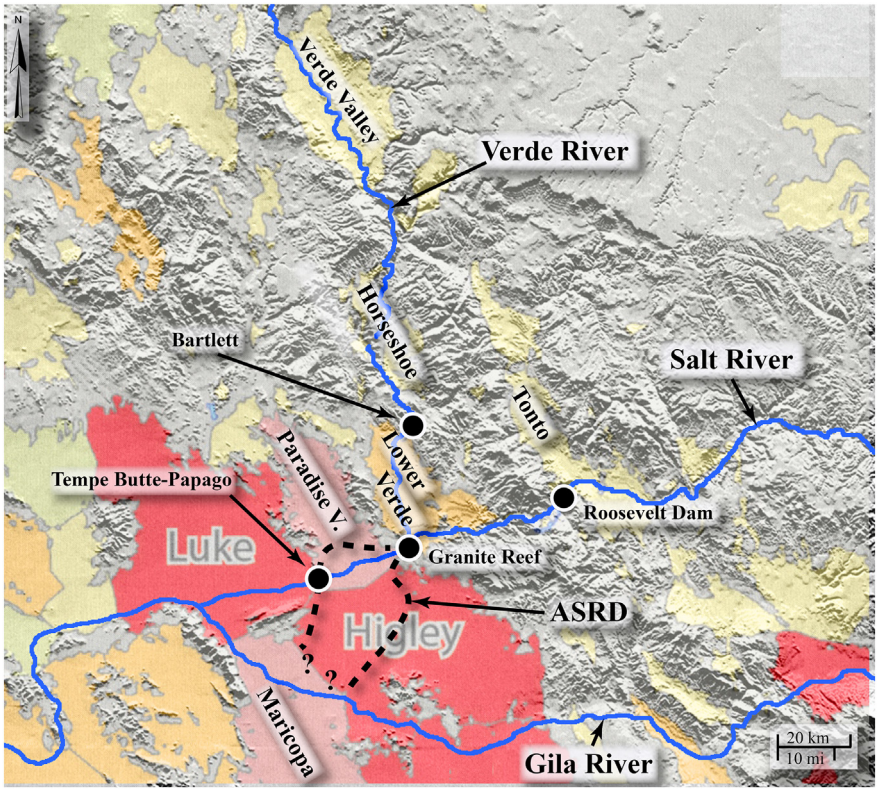

Fig. 2. Modern positions of the Verde, Salt and Gila rivers juxtaposed on extensional basins in central Arizona, where color reflects relative basin volume (highest red, then pink, orange, green and yellow) (Spencer, 2011b) and overlain on a U.S. Geological Survey shaded relief map. An inset box in Fig. 1 identifies the area of this figure. The ASRD stands for the ancestral Salt River deposits, identified by the dashed lines and mapped in detail elsewhere (Skotnicki and DePonty, 2020).

the eastern portion of the Phoenix, Arizona, metropolitan area in the Higley Basin (Skotnicki and DePonty, 2020). Well logs show an abrupt and distinct sedimentological contact separating non-Salt River, endorheic deposits below from ancestral Salt River deposits (ASRD) above. Distinct clast assemblages, along with an abrupt contact between them, indicate the sudden arrival of an exotic river — the newly integrated Salt River, a hypothesis proposed in prior research (Laney and Hahn, 1986).

Superimposition requires a mass of easily erodible material (i.e., cover mass) that overlies geologic or topographic structures that are later traversed as the river is "let down" over those structures as the cover mass erodes. This process would require a pre-existing river flowing over transverse structures. No evidence exists of cover mass or far traveled material in Higley Basin endorheic deposits (Skotnicki and DePonty, 2020).

An argument for stream piracy by headward extension has been evoked as a possible mechanism to integrate basins within the greater Gila River drainage basin (Dickinson, 2015), despite broad questions in the literature regarding the efficacy, efficiency, and general misconceptions of this process (Bishop, 1995; Douglass and Schmeeckle, 2007; Seong et al., 2016b; Larson et al., 2016; Gootee et al., 2020; Dorn et al., 2020). In this argument, a fortuitous gully erodes headward prior to the establishment of a river flowing through the landscape. A headward eroding channel then captures a higher hydrologic system and reroutes it down a new course. Conceptually, this bottom-up argument for the integration of the Salt and Verde rivers has problems in that there was no pre-existing drainage to provide the erosional capacity to erode headward, over several dozen kilometers, through competent substrate and mountain ranges.

As in other cases of drainage integration, extensional tectonic terrains in the BRP seem to involve sediment infilling closed depressions and often followed by lake overflow (Connell et al., 2005; Spencer, 2011a; Ren et al., 2014; Pearthree and House, 2014; Repasch et al., 2017; Meek, 2020). This is certainly the case for the Salt and Verde rivers, where water and sediment was impounded in the form of perennial lakes, playas, and basin fill (Lance et al., 1962; Bressler and Butler, 1978; Anderson and Piety, 1987; Anderson and Piety, 1988; Scarborough, 1989; Spencer et al., 2001; Hildabrand, 2015) in the Tonto, Horseshoe, and Verde Valley basins (Figs. 2 and 3).

Others have argued previously that the presence of large upstream basins filled with abundant fine-grained lake deposits — subsequently eroded and exhumed — provide evidence for top-down drainage integration via basin overflow as the most reasonable explanation for the formation of the Salt River (Douglass et al., 2009a; Larson et al., 2010; Larson et al., 2014; Larson et al., 2016). Of the four competing hypotheses used to explain transverse drainage development, prior evidence is most consistent with the lake overflow hypothesis for the initiation of through-flowing Salt and Verde rivers (Table 1).

1.2. Geological setting

The BRP in central Arizona began forming in the Oligocene (Eaton, 1982; Spencer et al., 2001; Chapman et al., 2019), one of several large areas of western North America that experienced widespread extension and faulting. High heat flow and high strain rates in central Arizona led to rapid extension along low-angle normal faults during the early Miocene (Spencer and Reynolds, 1989). These detachment faults are exposed in metamorphic core complexes (Reynolds, 1985) and project under various parts of the Higley and Luke basins. The middle to late Miocene saw the region experience crustal cooling, where high-angle normal faults produced subsiding grabens and half-grabens that then accumulated great thicknesses of sediment eroded from the nearby mountains (Scarborough, 1989).

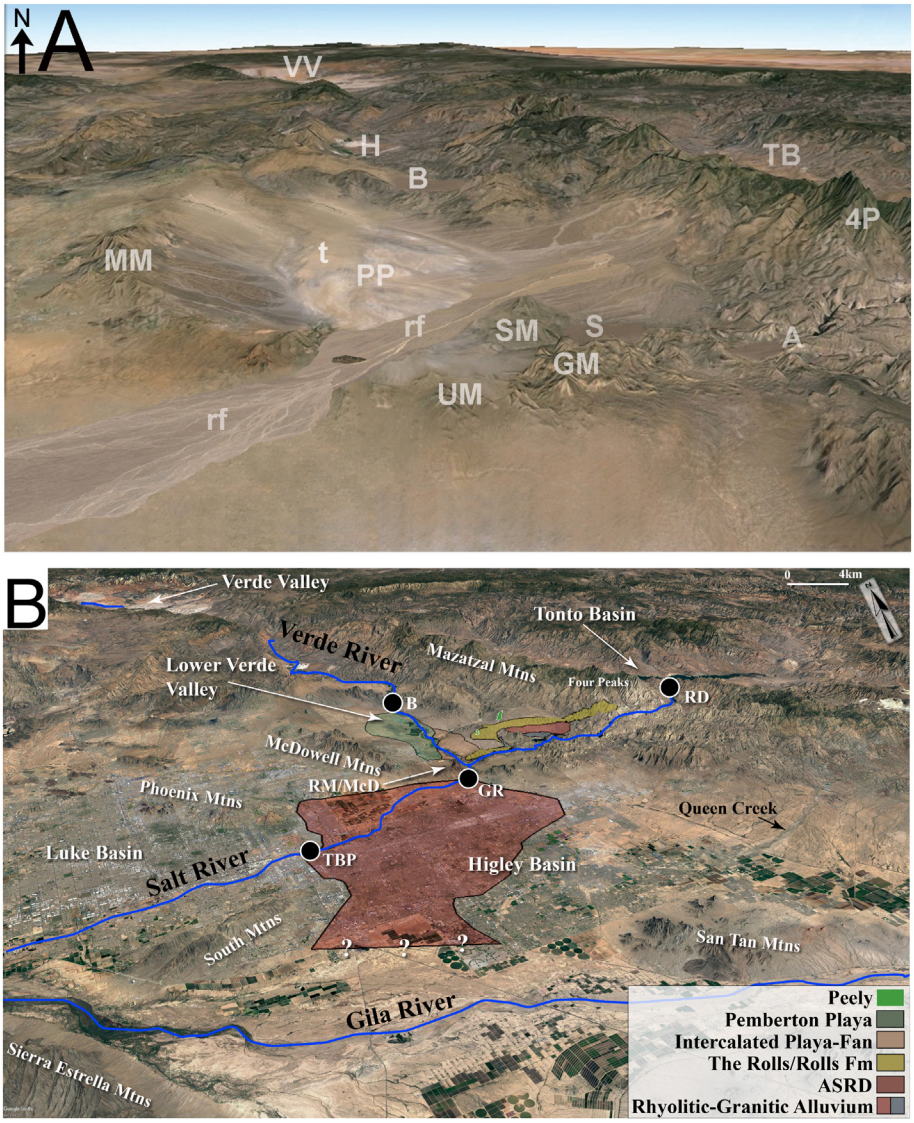

Fig. 3. Locations discussed in the paper viewed through two oblique perspectives. (A) An artistic reconstruction of the topography ca. 3.3 Ma centered on the lower Verde River valley. (B) Northeast-looking annotated Google Earth image of the entire metropolitan Phoenix area and higher mountainous topography to the north and east; the location of this frame is presented in Fig. 1. Locations discussed in the paper are identified by the following abbreviations: 4P (Four Peaks area of the Mazatzal Mountains); A (Apache reservoir); ASRD (ancestral Salt River deposits); B (Bartlett reservoir); GR (Granite Reef Dam); GM (Goldfield Mountains); H (Horseshoe reservoir); MM (Mount McDowell); TBP (Tempe Butte Papago bedrock ridge); PP (Pemberton playa); RD (Roosevelt Dam); rf (Rolls formation); RM/McD (Red Mountain/Mount McDowell); S (Saguaro reservoir); SM (Stewart Mountain);t (tephra site for Nomlaki tuff); UM (Usery Mountains); and VV (Verde Valley).

As active faulting and extension probably started to slow in late Miocene, basins filled towards capacity and developed relatively flat, low-relief valley floors (Menges and Pearthree, 1983). However, at least three young faults with presumed or demonstrable late Quaternary offset are exposed north and east of the LVRV (Pearthree and Scarborough, 1985). The Horseshoe and Sugarloaf faults both form the western structural boundary of two large half grabens. The Carefree fault is more cryptic but also may form a southern structural boundary to the Carefree Basin (Leighty et al., 1997). These faults all lie along the very northeastern edge of Arizona's BRP. Farther south, however, no Quaternary-age faults have been identified within the study area. Fanning-dip sediments within middle to late Tertiary sedimentary deposits north of Saguaro Lake (Skotnicki and Leighty, 1997) and southwest of Bartlett Lake (Skotnicki, 1996), and the presence of extensive flat-lying playa deposits within the LVRV indicate that faulting waned probably near the beginning of the Pliocene. Minimal tectonic activity in the Pliocene is also supported by evidence in the eastern Higley Basin, identified by Gootee (2013).

Exposed lithologies in the study area display a complex mix of rock types and ages (Fig. 4). Extrusive volcanics of Neogene age outcrop as basalts and also felsic eruptions from calderas. These extrusive rock types, as well as the metamorphic Pinal Schist and Precambrian rocks, can produce a wide range of sediment sizes in ephemeral washes from boulders to clay. Granitic rock types, in contrast, generate much of the sand observed in the drainage networks of the region.

2. Landscape prior to exotic rivers

2.1. Summary

The late Pliocene landscape prior to Salt River drainage integration included the Verde Valley and Tonto basins (Fig. 2) that held perennial lakes (Bressler and Butler, 1978; Anderson and Piety, 1988; Scarborough, 1989; Spencer et al., 2001). Lower elevation endorheic

Table 1
Evidence for lake overflow of the Salt and Verde rivers based on geomorphic transverse drainage criteria (Douglass et al., 2009b; Douglass et al., 2009a).

Transverse drainage criteria	Roosevelt Dam Canyon across Mazatzal Mountains (Salt River)	Bartlett Dam Canyon across the Needles (Verde River)
Faulting or uplift age of the bedrock high	Tonto Basin, immediately upstream of Roosevelt Dam, resulted from Basin and Range faulting and is infilled with a mix of Pliocene lacustrine and terrestrial sediments (Lance et al., 1962; Anderson and Piety, 1988). The Salt River extended into the Tonto Basin after lacustrine deposition, indicating the Salt River post-dates uplift of the bedrock high (Potochnik, 1989).	The Bartlett Basin, immediately upstream of Bartlett Dam, resulted from Basin and Range faulting (Skotnicki, 1996) that predates Verde River (Bressler and Butler, 1978; Pearthree, 1993)
Evidence of a covermass	None observed	None observed
Structural control asymmetry of the transverse drainage across the bedrock high	None observed	None observed
Multiple transverse drainages across the bedrock high (including the presence of wind gaps along the bedrock high)	None observed	None observed
Topographic control of transverse drainage incision into the bedrock high (accounting for deflected and ponded antecedent drainages and partial burial of the bedrock high for superimposed drainages)	None observed	None observed
Offset or flexed depositional or strath terraces along the bedrock high (assuming no post-transverse drainage incision deformation)	None observed	None observed
Transverse drainage sediments deposited atop the bedrock high	None observed	None observed
Ponded deposits upstream and below the rim of the bedrock high	The Tonto Basin deposits represent Pliocene lacustrine deposition upstream of the bedrock high (Lance et al., 1962).	Bressler and Butler (1978) indicate deposition ceased ca. 2.5 Ma
Paleo-shorelines upstream of the bedrock high	None observed	None observed
Fluvial sediments downstream of the bedrock high that record rapid arrival of the upstream drainage or continually deposited gravels that record erosion into the bedrock high	Basalt gravels sourced to the overflow of the Tonto Basin arrive suddenly in the ancestral Salt River gravels in the Higley Basin (Skotnicki and DePonty, 2020; Dorn et al., 2020). Also, Mescal limestone sources to the overflow near modern day Roosevelt Dam are mixed with Rolls formation sediment to form a strath "Stewart Mountain" terrace (Dorn et al., 2020)	Basalt gravels sourced to the overflow of the Bartlett Basin arrive suddenly in the ancestral Salt River gravels in the Higley Basin (Dorn et al., 2020)
Sedimentological evidence that water extended downstream of the bedrock high prior to fluvial sediments sourced upstream of the bedrock high	None observed	None observed
Presence of fault scarps or other related tectonic landforms along the bedrock high (assuming no post-transverse drainage incision deformation)	None observed	None observed
Topographic indication of a paleo-basin upstream of the bedrock high	The Tonto Basin extends upstream of the bedrock high of the Mazatzal Mountains	Bartlett Basin extends upstream of the bedrock high composed of the Needles Formation materials (Skotnicki, 1996). In addition, upstream, Horseshoe was a paleobasin as was the Verde Valley that hosted a freshwater lake (Hildabrand, 2015) before its emptying
Elbow of capture just upstream of the bedrock high	A possible elbow of capture upstream of the bedrock high	None observed
A gravel capped drainage divide, with an associated paleo flow direction of the transverse drainage, immediately upstream of the bedrock high	None observed	None observed

basins (and adjacent ranges) separated these lakes from the ocean with dry playas at their center. In the case of the Salt River (Fig. 2), a newly integrated stream would have to find a way to breach the Tonto Basin, then cross the LVRV, the Higley Basin, Maricopa Basin, and Luke Basin to establish its present course. These basins were closed as late as 3.3 Ma, when Nomlaki tuff accumulated in Pemberton playa of the LVRV (Dorn et al., 2020).

At some point during the middle or early Pliocene, the LVRV reached a condition of sediment overfill. We hypothesize here that a ramp of alluvial-fan sediment (called here the Rolls formation) originated in the Mazatzal Mountains (Fig. 3b) and formed a topographic and sedimentological connection between two endorheic basins (LVRV and the Higley Basin in Figs. 2 and 3b). The fanglomerate ramped over a bedrock sill near Granite Reef Dam (Figs. 2–4). When water started flowing in the Salt River over the Roosevelt Dam bedrock sill (Fig. 4), the discharge flowed on top of the pre-existing alluvial-fan ramp into the topographically lower Higley Basin —modern-day location of eastern metropolitan Phoenix.

2.2. Pre-integration landscape of the Higley Basin, eastern metropolitan Phoenix, Arizona

The Salt and Verde rivers currently discharge into the LVRV and then flow across a bedrock divide near modern-day Granite Reef Dam into the Higley Basin (Figs. 2–5), a basin that is filled with more than 3000 m of sediment at its deepest. Most water wells have only been drilled into the uppermost 460 m, so sparse information currently exists below this depth. Other than the alluvial fan-ramp discussed in Section 2.1, the endorheic Higley Basin was being filled with locally-sourced sediments laid down by small drainages that eroded the surrounding bedrock mountains (Fig. 4). Queen Creek (Fig. 3B) was among the largest (Gootee et al., 2020) of these local drainages.

Gootee et al. (2020) investigation of Queen Creek reveals a consistent clast assemblage throughout the Pliocene and Quaternary. This indicates that the Queen Creek drainage basin itself did not show significant enlargement from headward erosion — a finding inconsistent with the hypothesis proposed for the Gila River system as a whole (Dickinson, 2015). Queen Creek more accurately reflects the

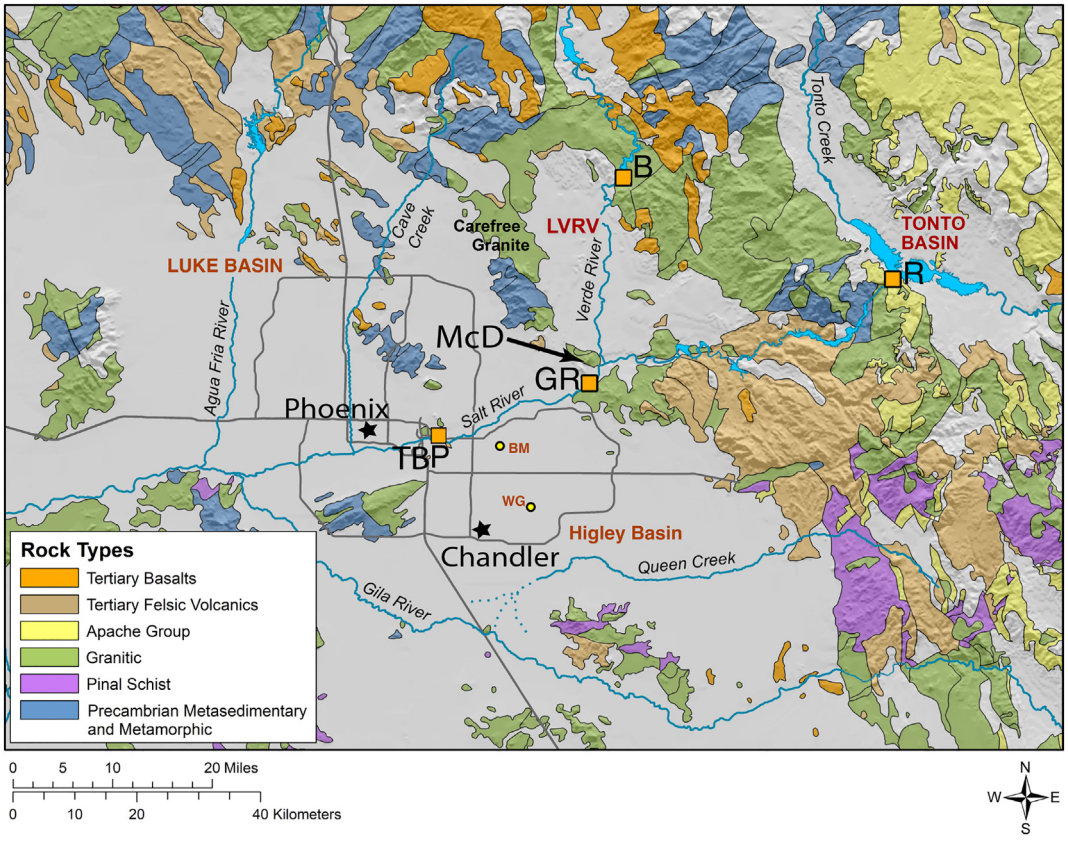

Fig. 4. Basic geological map of the study region, adapted from Richard et al. (2002). Small yellow circles identify locations of wells sampled for cosmogenic burial dating near the intersections of Brown and Mesa (BM) and Warner and Gilbert (WG) roads. Four squares identify bedrock sills that rivers had to cross in order to integrate basins and create a transverse drainage: R near Roosevelt Dam; B near Bartlett Dam; GR near Granite Reef Dam; and TBP, between Papago Park on the north side of the Salt River and Tempe Butte on the south side of the river. Each separates bedrock basins: B is the low point between the LVRV and the small basin occupied by Bartlett lake; R is the low point between Tonto Basin and the lower Verde River valley (LVRV); GR is the low point between the LVRV and the Higley Basin; TBP is the low point on a Papago bedrock ridge separating the Higley and Luke basins. Also noted on this figure are McD (Red Mountain/McDowell Mountain) and the city of Chandler, Arizona, to provide spatial context for Fig. 11.

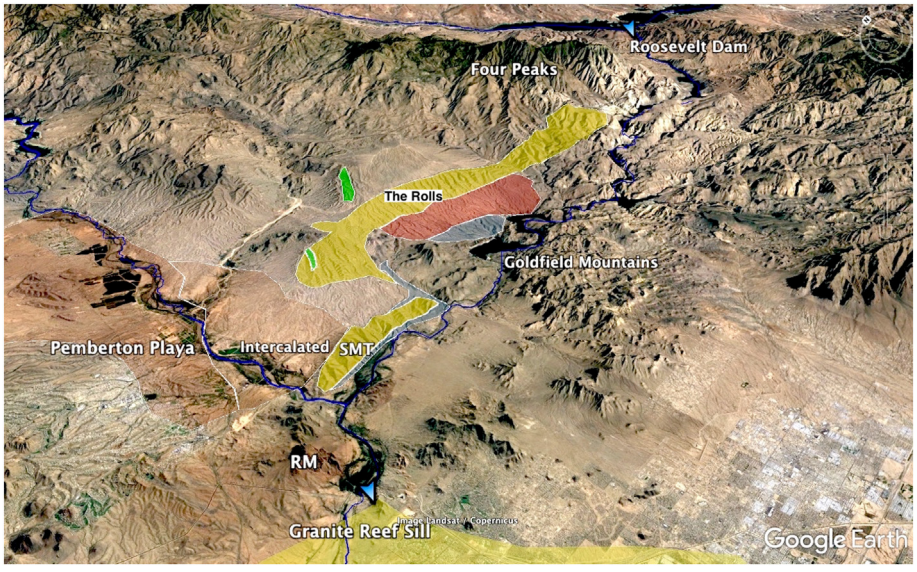

Fig. 5. Simplified map of Pliocene sediments in the LVRV based on geologic mapping by the first author and confirmed independently by the second author. This map can also be found as online supplemental KML file. The mapping units are polygons on a Google Earth northeast-looking view, with a scale perspective provided by horizontal distance of 50 km from the Granite Reef Sill to Roosevelt Dam. One blue arrow indicates the location of the spillover sill at the present-day location of Roosevelt Dam, and the other indicates the present-day location of the bedrock sill at Granite Reef Dam. RM indicates the location of Mount McDowell (locally known as "Red Mountains"). There are two main exposed pieces to the Rf: closest to Four Peaks called The Rolls and the SMT. Two identified alluvial-fan units predate the Rolls formation: a rhyolite-rich clast assemblage (brick red) and the granitic feldspar-rich sediment (gray); fanglomerate derived from Mt. Peeley (green) overlies the Rf.

general behavior of endorheic drainages in the region: an areic stream produced an alluvial fan (Fig. 3B) that required high magnitude flood events to extend sediment out onto the floor of the Higley Basin (Gootee et al., 2020).

2.3. Landscape of the lower Verde River valley

The LVRV plays an important role in unraveling geomorphic processes and events associated with drainage integration, for several reasons. It occupies a position immediately downstream of hypothesized lake overflow sites near present-day Bartlett Dam on the Verde River and Roosevelt Dam on the Salt River (Figs. 2–4). The LVRV hosts the confluence of the Salt and Verde rivers, contains preserved pre-integration playa remnants that contain the Nomlaki 3.3 Ma tephra (Dorn et al., 2020), and contains erosional remnants of adjusting pediments (Larson et al., 2017; Larson et al., 2020), alluvial fans (Skotnicki and Leighty, 1997; Skotnicki, 2000; Larson et al., 2020), and stream terraces (Pope, 1974; Péwé, 1978; Larson et al., 2010; Seong et al., 2016a; Larson et al., 2017; Larson et al., 2020).

2.4. The Rolls formation precursor to Salt River deposits

The ASRD (Fig. 3B) represents the initial arrival and subsequent aggradation of a newly integrated Salt River system in the Higley Basin (Skotnicki and DePonty, 2020). Analyses of clast assemblages obtained in cuttings from wells drilled throughout the Higley Basin (Skotnicki and DePonty, 2020) reveal ASRD deposits are dominated by >80% metamorphic clasts and the particle size is uniformly gravel or larger.

These characteristics of the ASRD are distinctly different than the underlying unit. The unit below the ASRD (Fig. 3) typically contains <25% dark, fine-grained metamorphic clasts with conspicuous large feldspar grains and quartz grains. These pre-ASRD sediments do not appear to have an obvious source of bedrock in any of the mountains surrounding the Higley Basin. Yet, materials underneath the ASRD were identified by Laney and Hahn (1986) as closed-basin deposits, a finding confirmed by Skotnicki and DePonty (2020).

Because the pre-ASRD sediments in the Higley Basin had substantial components not derived from a local source within the Higley Basin, fieldwork was conducted in the upstream LVRV basin in an attempt to find a source. One location where surficial deposits were investigated was previously identified as a newly discovered Salt River terrace, the "Stewart Mountain terrace" (SMT; Fig. 5; Larson et al., 2010). The SMT is a gently sloping (~E-W) dissected plateau that rests approximately 60 m above the next highest Salt River terrace. The SMT was originally interpreted as an aggradational fill terrace (Larson et al., 2010).

Little is known about the internal sedimentology and structure of the SMT beneath the terrace surface and above underlying Neogene basin fill. This is largely because of the lack of clean vertical exposures and geophysical data. However, fieldwork in this study suggests the provenance of the SMT clast assemblage is very much like that of the pre-ASRD unit underlying ASRD sediments in the Higley Basin. In addition, another lithologically similar clast assemblage is found in a nearby area called "The Rolls" (Figs. 3 and 5), that displays a distinctive topography on the piedmont below the Four Peaks of the Mazatzal Mountains. No other known deposits in the region contain material that matches this clast assemblage.

Based on the currently recognized outcrop pattern, these sediments likely originate from near Four Peaks (Figs. 3 and 5). A distinctive and diagnostic rock type present in the sediments occurs within a contact aureole surrounding the north side of Four Peaks (Powicki, 1996; Skotnicki, 2000): a dark gray metamorphosed psammite that contains abundant and distinctive porphyroblasts of fine-grained clots of dark biotite and lighter clots of muscovite after andalusite. These unique rocks have no other known source other than the immediate north and west sides of Four Peaks. The Apache Group is a set of Mesoproterozoic geological formations in the region including the Troy Quartzite, the Mescal Limestone, the Dripping Spring Quartzite, and the Pioneer Shale. Although the Rolls formation contains some Proterozoic Apache Group clasts, they are much less abundant than the Apache Group clasts found within the fully integrated Salt River sediments like the ASRD and topographically lower Salt River terraces. Also, the majority of clasts of all rock types within these deposits are subangular to subrounded and poorly sorted, which is quite different than the well-rounded sediment of the ASRD and the sediments within the modern Salt River.

The area labeled on "The Rolls" on USGS 1:24,000 7.5 minute quadrangles forms an elongate band of topographically elevated hills bordered on the north and south by recessively eroding deposits containing granitic clasts and quartz/feldspar grus, and clasts of Neogene rhyolite, respectively. This elevated band of hills exemplifies relief inversion, where a formerly topographically lower alluvial-fan deposit is now higher in the landscape because its larger particle sizes and metamorphic clasts are more resistant to erosion than the underlying rhyolite-rich fan deposits. The Rolls aligns with a series of isolated and dissected deposits to the east. We informally name the deposit, and other deposits downstream with similar clast assemblages, the "Rolls formation" (informal abbreviation of Rf).

We interpret the above evidence to suggest that Rf deposits pre-date the ASRD and did not excavate the same lithologic source as the fully integrated Salt River, a conclusion consistent with detrital zircon analyses from the Rf and the ASRD (Dorn et al., 2020). We interpret the material underneath the surface of the SMT to be the same as the Higley Basin's pre-ASRD unit (Skotnicki and DePonty, 2020). We hypothesize that the outcrop pattern shown in Fig. 5 suggests that the drainage that deposited the Rf formed a pre-Salt River alluvial fan whose axis was on the southern margin of the LVRV and spilled over into the Higley Basin (Fig. 3A).

Evidence from the SMT also suggests the Salt River did occupy and likely reworked the Rolls formation fanglomerate. The surface of the SMT contains sparse, but exotic cobble-size clasts of Mescal Limestone intermixed with the Rf clast assemblage (Dorn et al., 2020). The most likely and proximal source for Mescal Limestone comes from outcrops adjacent to and south of Roosevelt Dam (Spencer and Richard, 1999) in the Tonto Basin (Figs. 3–5). Rf deposits elsewhere contain no observable clasts of Mescal Limestone. Our interpretation is that the knickpoint initiated by lake overflow at the outlet of Tonto Basin (Douglass et al., 2009a) retreated headward allowing the Mescal Limestone to erode and be incorporated into the flow of the newly integrated Salt River. Clasts of the Salt River were then mixed with Rf fanglomerate as the river flowed across it. The existence of Mescal Limestone on the SMT also provides an important minimum topographic indicator of the position of the Salt River when it first entered the LVRV. Future geophysical surveys and sedimentological analysis at depth across the spatial extent of the Rf, and particularly within the SMT would be required to support or refute this hypothesis.

Another aspect of the LVRV highlighted in Fig. 5 is the coexistence of the Rf as an alluvial-fan ramp over the Granite Reef bedrock sill and the Pemberton playa. Between the Pemberton playa and the Rolls formation was a zone of intercalation of the finer fraction of alluvial materials (small gravel to fine sand) and playa silt and clay. The boundary between these materials can be seen to shift horizontally and vertically in exposures throughout the "intercalated" mapped area (Figs. 3 and 5).

2.5. Analogs for the fan ramp hypothesis

Extensional basins that fill with sediment may eventually reach an overfill condition (Flemings and Jordan, 1989; Catuneanu, 2004; Dickinson, 2015; McGlue et al., 2016). We hypothesize that this occurred in the LVRV in the Pliocene when the Rf alluvial fan prograded across the Granite Reef sill into the Higley Basin. During this overspill of fanglomerate, an adjacent Pemberton playa co existed in the LVRV.

Towards the end of the Pliocene, Nomlaki tuff was deposited on the playa and then incorporated into sediment ~3.3 Ma (Dorn et al., 2020).

An overfill condition and the presence of a playa is not a contradiction. Closed endorheic basins in other extensional tectonic settings also contain both playas and alluvial fans that ramp fanglomerate across bedrock sills (Fig. 6B–D) — all in a geomorphic setting without an exoreic through-flowing stream. An artistic illustration presents how the LVRV might have looked at 3.3 Ma (Fig. 6A) when the Nomlaki tuff was deposited on the LVRV playa (Dorn et al., 2020). In our hypothesis, the Rolls formation fanglomerate spilled sediment across the low bedrock divide near modern-day Granite Reef Dam (Fig. 5), all while the Higley Basin remained endorheic without the presence of the Salt River.

3. Dating the ASRD and the arrival of an exoreic river

3.1. Cosmogenic burial dating methods

Prior researchers have acquired samples from drilling operations for cosmogenic burial dating (Balco et al., 2005), but our efforts to understand the timing of drainage integration used well cuttings more extensively than prior studies and from an array of well drilling operations at a variety of depths across an entire basin. Drill cuttings collected within the ASRD were originally cobbles to large boulders that were subsequently ground up into smaller fragments by the drilling process; these fragments were collected in buckets.

We largely rely on isochron burial ages. Although single burial ages provide a maximum-limiting age, the isochron approach provides greater precision (Balco and Rovey, 2008). Sampling focused on cuttings from two wells (Fig. 4): near the intersection of Brown and Mesa (BM) roads (33.4366, −111.8233) and another near the intersection of Warner and Gilbert (WG) roads (33.3356, −111.7889).

We also use one sample of well cuttings collected by prior researchers (Reynolds and Bartlett, 2002). This prior work recognized the sudden arrival of the Salt River near the present-day location of the Phoenix Sky Harbor Airport by examining wells drilled to study a contaminant spill in groundwater (Reynolds and Bartlett, 2002). In response to ASRD aggradation (Skotnicki and DePonty, 2020), the Salt River spilled across the Papago bedrock ridge (Figs. 3B and 4), and this single burial age comes from Salt River gravels just above the contact with the underlying basin fill.

We also obtained samples from two crucial geomorphic settings that would provide further insight into the timing of integration along the Verde River within the LVRV (Figs. 2–4). The Verde River deposited alluvium immediately downstream of where it integrated across a bedrock sill near Bartlett Dam (Figs. 2–4). These Verde River gravels (33.6772, −111.6975) occur in the fill of the highest Verde River deposit, the Lousley Hills river terrace (Seong et al., 2016a). Also, aggradation of these gravels blocked flow of local pediment tributary streams resulting in aggradation (Fig. 7) (33.6893, −111.7395) of a wedge of grus-derived alluvium (Larson et al., 2020).

All samples were prepared in the Cosmogenic Nuclides Laboratory of Korea University (Seong et al., 2016b), following normal community processes (Kohl and Nishiizumi, 1992). Crushing samples was followed by sieving to 250–500 μm. Treatment with HF-HNO_3 removed meteoric Be and organic matter, followed by addition of ~400 μg of low ($<10^{-15}$ in $^{10/9}$Be) resolution ^{9}Be carrier. Be and Al were separated by ion exchange and precipitated at pH > 7. Beryllium and aluminum hydroxides were dried and converted to oxides and loaded into targets measured using 6MV Accelerator Mass Spectrometry (AMS) at the Korea Institute of Science and Technology (KIST), Seoul, Korea. AMS results were corrected for blanks (3×10^{-15} $^{10/9}$Be) and then converted into absolute concentration of ^{10}Be and ^{26}Al (Seong et al., 2016b).

We calculated all cosmogenic exposure ages using the CRONUS exposure age calculator version 2.3 (Balco et al., 2008). Simple burial dating is based on the difference in half-lives of ^{26}Al (0.705 Ma) and ^{10}Be

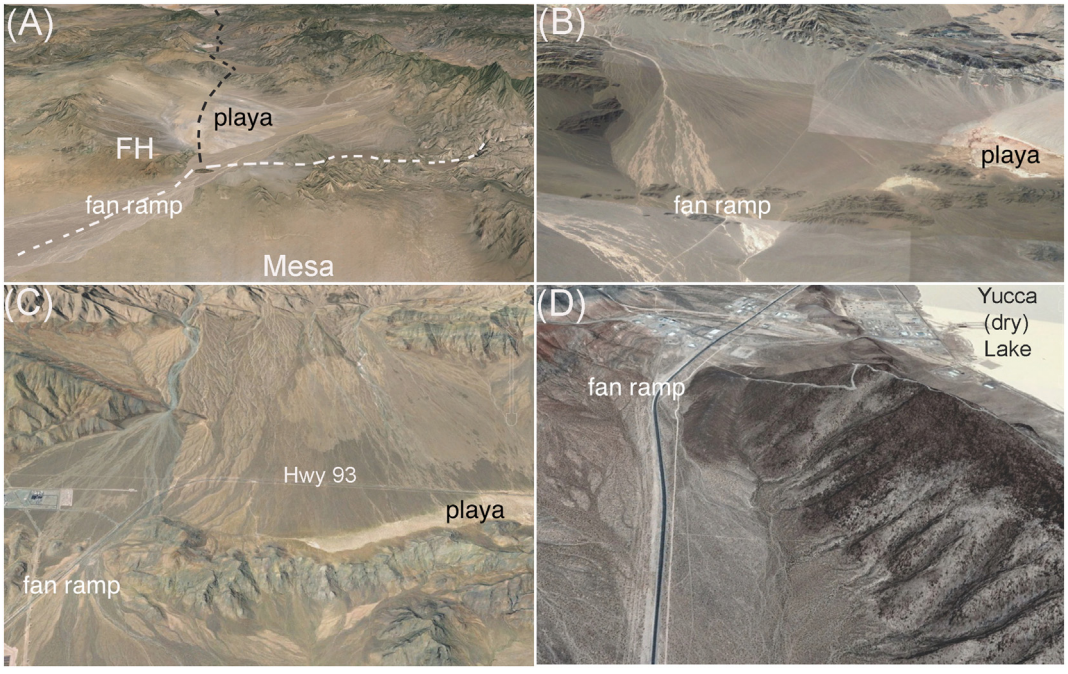

Fig. 6. Alluvial-fan spillovers of extensional tectonic basins concurrent with playas. (A) Artistic rendering of the Lower Verde River Valley's closed basin about 3.3 Ma prior to the arrival of the Salt (white dashes) and Verde (black dashes) rivers, using Google Earth north-looking image as a base. Note that the Rf alluvial fan spills over the bedrock sill near the present-day location of Granite Reef Dam just southeast of modern day Fountain Hills (FH), all while the Pemberton playa occupies a topographic low spot. (B) Mendoza Province in Argentina where an alluvial fan spills over a bedrock ridge, yet a playa still remains intact blocked by fan aggradation. (C) Arrow Canyon Range, Nevada, where an alluvial-fan system spills over a bedrock sill, positioning a playa in a topographic low. (D) Yucca Pass, Nevada, where alluvial-fan materials spill over a bedrock sill, while the Yucca (dry) Lake playa occupies the topographic low.

Fig. 7. The base of this exposure shows the top of the Pemberton playa deposit in the LVRV (Figs. 2 and 4). This playa deposit represents the formerly endorheic basin in the LVRV prior to Salt River and Verde River integration through this basin. The contact between the playa and overlying gravel-dominated sediment is now an unconformity. The overlying unit consists of sediment derived from the local McDowell Mountains a few kilometers distant that accumulated in response to Verde River aggradation following integration. Thus, this sediment post-dates Verde River integration.

(Chmeleff et al., 2010; Korschinek et al., 2010) assuming 6.8:1 for the initial ratio of $^{26}Al/^{10}Be$ (Granger and Muzikar, 2001). Considering the longevity of sediment transfer and evacuation from the source to the basin in dry area such as the Sonoran Desert, the burial age induced from single sample should be considered for maximum age because of inherited amounts of $^{26}Al/^{10}Be$. Thus, we applied isochron burial dating to some wells to infer a better estimation of true depositional age (Balco and Rovey, 2008; Erlanger et al., 2012). We followed the approach implemented by Erlanger et al. (2012). Where funding allowed, we used more than five sub-samples for an isochron to better constrain the depositional age — although some of the previous studies in the region used only 2–4 sub-samples to minimize cost (Jungers and Heimsath, 2016).

3.2. Cosmogenic burial dating results

Cosmogenic burial ages provide critical constraints on the timing of Salt and Verde river inception and evolution (Table 2). The presentation of results is organized chronologically, beginning with the 3.9 ± 0.7 Ma isochron burial age (Fig. 8) for gravels of basin fill underneath the ASRD in the BM well (Fig. 9). This age on this Rf material does not tightly constrain when the basin-fill deposition ceased because ~20 m of fine sediment inappropriate for dating rests on top of the analyzed sample. However, it does bracket the arrival of the Salt River, requiring it to be younger than 3.9 ± 0.7 Ma. This age is consistent with the occurrence of the 3.3 Ma Nomlaki tuff deposited in playa sediment of the LVRV as that, too, provides a maximum-limiting age for the end

Table 2
Cosmogenic ages related to the geomorphology of the Salt River (SR), and Verde River (VR).

Sample	Depth	Age (ka)	Error (ka)	No. aliquots	Method	Source
Blue Point strath terrace (SR)	Surface	35.6	17.6	5	Surface expos[a]	(Larson et al., 2017)
Mesa strath terrace (SR)	Surface	89.6	22.3	6	Surface expos[a]	(Larson et al., 2017)
Sawik strath terrace (SR)	Surface	333.4	22.2	6	Surface expos[a]	(Seong et al., 2016a)
Tributary Stoneman Wash (VR)	4 m	1645.3	82.2	2	Simple burial[b]	This study
Lousley Hills fill terrace (VR)	40 m	2185.4	1092	1	Simple burial[b]	This study
Sawik gravels at bedrock contact (SR)	4 m	691.9	34.5	1	Simple burial[b]	(Seong et al., 2016a)
Base of SR gravels Phoenix Airport	40 m	460.1	23	1	Simple burial[b]	This study
Brown & Mesa well (ASRD)	210 ft	2169.9	488.2	6	Isochron[c]	This study
Brown & Mesa (basin fill, pre-ASRD)	300 ft	3902.4	702.4	6	Isochron[c]	This study
Warner & Gilbert well (ASRD)	190 ft	547.4	120.4	2	Isochron[c]	This study
Warner & Gilbert well (ASRD)	280 ft	2773.0	512.9	4	Isochron[c]	This study
Knox & Alma School well (ASRD)	90–100 ft	836.0	41.8	1	Simple burial[b]	This study
Knox & Alma School well (ASRD)	200–210 ft	2208.2	110.4	1	Simple burial[b]	This study
Knox & Alma School well (ASRD)	270–280 ft	2104.7	145.6	1	Simple burial[b]	This study
Warmer & Val Vista well (ASRD)	150–160 ft	1383.3	55.7	1	Simple burial[b]	This study
Warmer & Val Vista well (ASRD)	300-310 ft	1466.0	41.6	1	Simple burial[b]	This study
Warmer & Val Vista well (ASRD)	340–350 ft	1700.6	685.0	1	Simple burial[b]	This study

[a] Simple surface exposure dating.
[b] Simple burial dating (maximum age).
[c] Isochron burial dating.

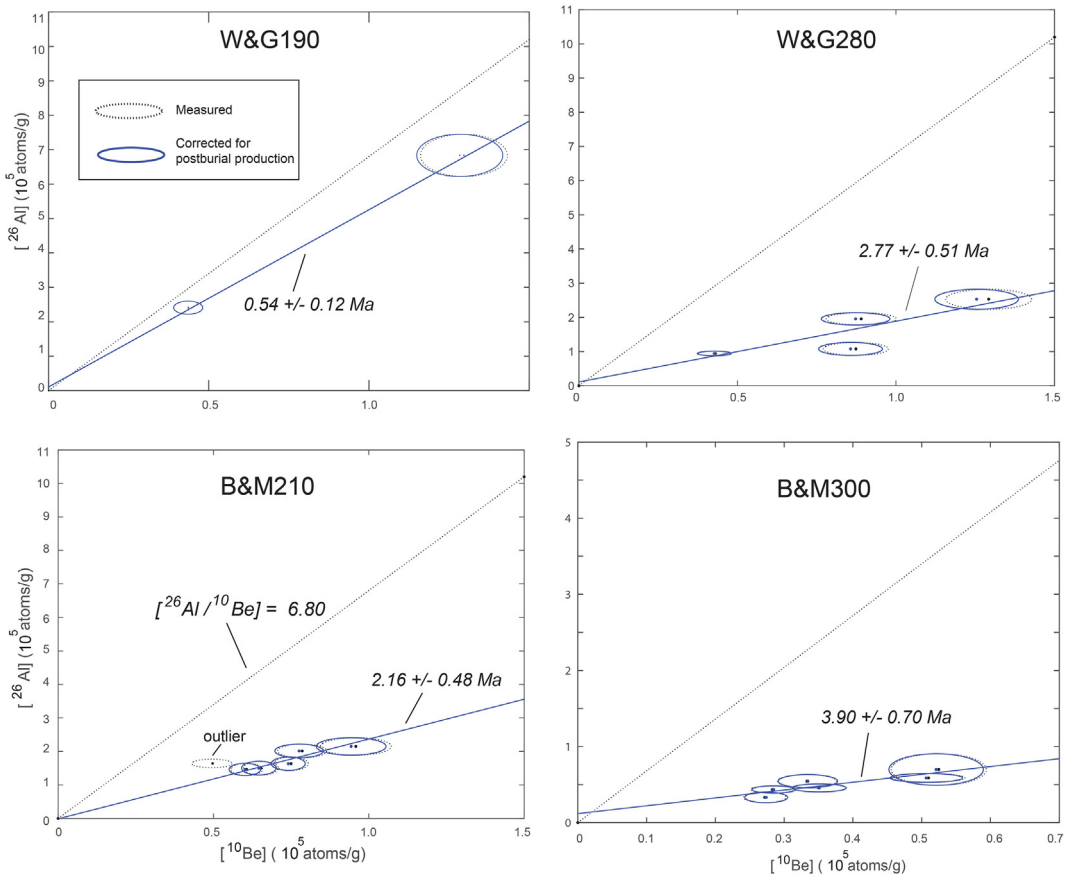

Fig. 8. Isochron plots for higher precision burial dating of key depths of well cuttings from the Brown and Mesa (B&M) well (Arizona Department of Water Resources well 55-223506) and Warner and Gilbert (W&G) well (ADWR 55-225424) (Skotnicki and DePonty, 2020). For the W&G well, the 190 ft. (58 m) depth is the middle of the ASRD, whereas the 280 ft. (85 m) depth is near the base of the ASRD. The BM well samples bracket the base of the ASRD at 210 ft. (64 m) and gravels at the top of the basin fill at 300 ft. (91 m).

of endorheic sedimentation along the Salt and Verde rivers (Dorn et al., 2020).

Fig. 8 presents isochron burial age plots for deposits near the base of the ASRD in the BM and WG wells identified in Fig. 4. Because well depths are sampled in 10 ft. (3 m) intervals, we report depths as they were recorded, in feet. The 210–220 ft. (65 m) depth in BM well at 2.16 ± 0.48 Ma and the 280–290 ft. (87 m) in the WG well at 2.77 ± 0.51 Ma provide the first known ages of Salt River deposits in the Higley Basin that constrain the timing of arrival of the Salt River. Fig. 9 superimposes the isochron ages (Fig. 8) on the mineralogic lith-logs (Skotnicki and DePonty, 2020) of the BM and WG wells. Sampling depths are not at the bottom of the ASRD, but rather the lowest sampling interval where we could be sure there was no contamination from basin fill material. Thus, the arrival of the Salt River at these locations would be older than the reported isochron dates. The age range of ~2.2–2.8 Ma for the deposits near the base of the ASRD could be a mixture of method uncertainties or the range could reflect lateral shifts in Salt River channel position over time. An isochron age for the middle of the ASRD and simple burial ages throughout the ASRD (Table 2) reveal that a major river deposited gravels for about 2 million years across a broad floodplain in the shape of what Skotnicki and DePonty (2020) interpret as a mega-alluvial fan.

Figs. 2 and 3B show the approximate location of the ASRD channels, the modern-day Salt River, and Tempe Butte-Papago bedrock ridge — the low point between the Higley and Luke basins. A sharp contact between endorheic basin-fill deposits and overlying cobbles of the Salt River reveals the sudden arrival of Salt River gravels just west of Phoenix's Sky Harbor Airport (Reynolds and Bartlett, 2002). One sample of cuttings from the base of the DM 512 well produced a single burial age of 460 ± 23 ka that is best interpreted as a maximum age for arrival of Salt River gravels (Table 2).

Seong et al. (2016a) sampled some of the highest deposits of the Salt River underneath the Sawik terrace ~25 km upstream of Phoenix's Sky Harbor Airport. They reported a burial age of 692 ± 35 ka (Seong et al., 2016a). This sample reveals that the Sawik-phase of the Salt River was transporting gravels at this site about 700 ka. Thus, based on available data in Table 2, we think that avulsion of the Salt River occurred at or after about 460 ka.

Our informal name for the stream that deposited the ASRD over a ~2 million year period is the "Sawik phase" of the Salt River, named for a prominent local topographic feature on the northern side of this ancestral version of the Salt River. We informally think of the Salt River taking its modern position only after the aggradational piracy (or aggradational spillover via a fluvial aggradation (Hilgendorft et al., 2020) process, as physically modeled in experiments (Douglass and Schmeeckle, 2007).

Aggradation of the ASRD from ca. 2.2–2.8 Ma until ca. 0.46 Ma raised the land surface high enough to allow the Salt River to flow over the low point between Tempe Butte and Papago Park at an elevation of approximately 326 m (1070 ft). When the Salt River arrived, the groundwater table was likely quite high. Then when the Salt River began to spill into the Luke Basin across the Papago Park bedrock ridge, it deposited ~30 m of gravels on top of ephemeral washes derived from nearby Papago Park (Reynolds and Bartlett, 2002).

The elevation of the Luke Basin just west of the airport was 293 m (Reynolds and Bartlett, 2002), and the elevation drop provided a steeper gradient than the Sawik version of the river east of this spillover point. By flowing westward instead of southward around South

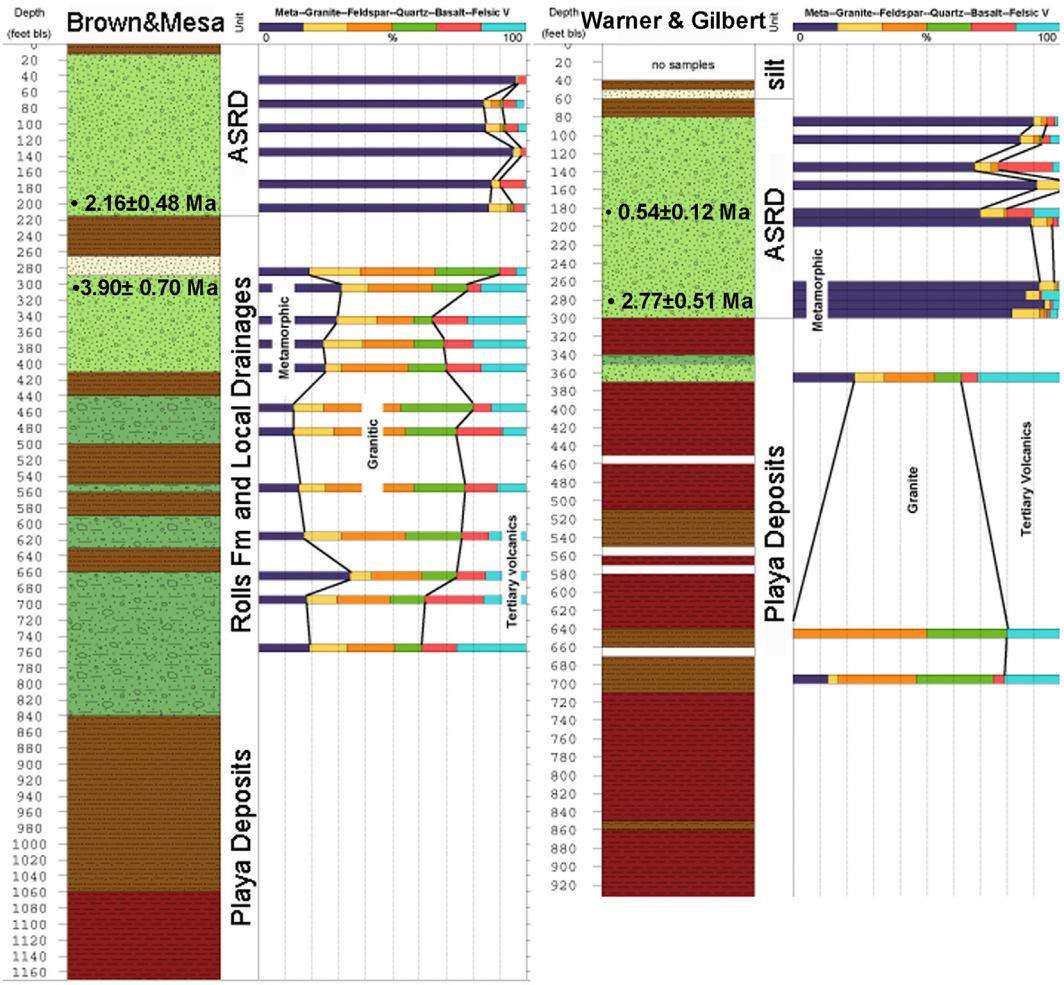

Fig. 9. Burial isochron ages on well cuttings from two sampled wells. The stratigraphy follows the style of mineralogical logs developed by S. Skotnicki where broad trends in rock type are visualized through bar graphs (Skotnicki and DePonty, 2020). For wells drilled into the ASRD, sometimes the ASRD is near the surface, and in other wells an eolian cover of silts deposited on top. Feet instead of meters are used in this graph because the wells are logged in feet and well-cutting samples are acquired in 10 ft. (3 m) intervals.

Mountain, the river length shortened by ~35 km. The combination of shortening and a knickpoint gradient likely led to incision into the Sawik-phase of the Salt River, creating the Sawik stream terrace (Péwé, 1978).

The incision of the Salt River into the ASRD is also consistent with the minimum ^{10}Be exposure age of ca. 333 ± 22 ka for the Sawik terrace (Seong et al., 2016a). Incision into the Sawik-age river channel likely dropped the water table considerably. The Salt River subsequently incised again at ~90 ka and then ~40 ka, producing the Mesa and Blue Point strath terraces, respectively (Larson et al., 2016). As Péwé (1978) originally observed, all three terraces are only found east of the location of aggradational piracy at the Papago bedrock ridge.

3.3. Meteoric ^{10}Be analyses of calcrete at the avulsion site

The hypothesis proposed by Skotnicki and DePonty (2020) is that aggradation of Salt River deposits allowed the river to reach the elevation of a low point in a bedrock ridge situated between Papago Park and Tempe Butte (Figs. 3–4). Two hundred meters away is a modern-day railroad cut that exposes a massive (>3 m thick) calcrete duricrust that cements cobbles and boulders of colluvium derived from a Neogene andesite porphyry lava flow on top of Tempe Butte. This "Tempe Butte" calcrete exposure was where we examined a ^{10}Be/^{9}Be profile to better understand groundwater changes through time at this location.

In contrast to in situ ^{10}Be used in burial dating, meteoric ^{10}Be (half-life: 1.387 × 10^{6} yr (Chmeleff et al., 2010; Korschinek et al., 2010) is more like ^{14}C in that it is produced in the atmosphere by cosmic ray interactions and delivered to Earth's surface by wet and dry fall out. Geomorphological applications of meteoric ^{10}Be include calculation of sediment or soil ages (Valletta et al., 2015) and erosion rates from surface soil and catchment-wide denudation rates (von Blanckenburg et al., 2012), but meteoric ^{10}Be has never been tested as such in calcrete.

A key methodological issue in the use of meteoric ^{10}Be involves the retention behavior of Be that is firmly adsorbed onto particles only when in a solution pH > 6 (Willenbring and von Blanckenburg, 2010). Retention is also dependent on grain size (Willenbring and von Blanckenburg, 2010). Those issues can be circumvented by normalization with a stable isotope ^{9}Be: ^{10}Be/^{9}Be ratio extracted from "reactive" phase (^{10}Be/^{9}Be$_{reac}$) indicating Be adsorbed onto mineral surfaces and precipitated in secondary solids (von Blanckenburg et al., 2012) like calcrete.

A total of five samples from the Tempe Butte calcrete (~3 m thick) were taken for Be isotope analyses (Table 3 and Fig. 10). We used a hybrid method to extract the reactive phase of Be (Jeong et al., 2018). After drying samples, we removed the >2 mm fraction to minimize size dependency of Be. Then, we extracted ^{10}Be$_{reac}$ by sequential leaching techniques (Bourlès et al., 1989). To measure the ^{9}Be$_{reac}$ concentration in the leached solution, we sub-sampled the solution and measured the concentration using Inductively Coupled Plasma Optical Emission Spectrometry (ICP-OES). ^{9}Be carrier was added to remaining solution, then

Table 3
Analytical results of meteoric ^{10}Be and $^{10}Be/^{9}Be$ profile of Tempe Butte calcrete.

Sample	Depth (m)	Sample mass (g)	Be carrier (mg)	$^{9}Be_{reac}$ concentration[a] (ppm)	$^{10}Be_{reac}$ concentration[b, c, d] (10^{7} atoms g^{-1})	$(^{10}Be/^{9}Be)_{reac}$[b] ($\times 10^{-9}$)
TBC001	0.00	1.0097	0.4270	0.15±0.46	3.37±0.03	3.37±0.03
TBC002	0.18	0.9840	0.4377	0.16±0.23	2.13±0.02	1.98±0.02
TBC003	0.91	1.0033	0.4400	0.22±0.12	1.61±0.02	1.13±0.01
TBC004	1.83	0.9871	0.4490	0.27±0.07	2.67±0.03	1.45±0.02
TBC005	2.74	0.9886	0.4455	0.24±0.24	2.05±0.02	1.26±0.01

[a] The reactive ^{9}Be concentrations were measured by inductively coupled plasma optical emission spectroscopy (ICP-OES).
[b] Propagated uncertainties from uncertainties in blank, Be carrier and AMS analytical error.
[c] A mean blank value (n = 4) of $5.29 \pm 2.43 \times 10^{-15}$ $^{10}Be/^{9}Be$ ratio was used to correct for carrier background.
[d] Isotope ratios were normalized to the ICN standard 5–1 with a ratio of 2.709×10^{-11}.

a potassium bifluoride fusion procedure (Stone, 1998) was carried out to successfully achieve isotopic equilibrium between ^{10}Be and ^{9}Be. The ^{10}Be and the $^{10}Be/^{9}Be$ ratio were measured by 6MV AMS at the Korea Institute of Science and Technology (KIST).

The $^{10}Be/^{9}Be_{reac}$ profile of the calcrete at Tempe Butte (Fig. 10C) indicates that the two different types of calcrete formed at very different times. $^{10}Be/^{9}Be_{reac}$ ratios for the three lowest samples of groundwater calcrete (Table 3) are essentially equivalent, where this massive calcrete formed through ongoing evaporation of groundwater, perhaps by capillary water movement (Fig. 10A).

The groundwater diagramed in Fig. 10B would have been caused by the presence of the ancestral Salt River as it aggraded near and at this location (Skotnicki and DePonty, 2020) (Figs. 8–9 and Table 2). Integration of the Salt River across the Tempe Butte-Papago sill is hypothesized to have dropped the water table, and this would have led to a change in carbonate deposition to pedogenic carbonate formation that has a very different $^{10}Be/^{9}Be_{reac}$ ratio in the upper 0.2 m.

Using $^{10}Be/^{9}Be_{reac}$, we calculated an order of magnitude in difference of ages for the groundwater and pedogenic calcretes in the profile illustrated in Fig. 10C. Unfortunately, the ability to obtain firm ages is not possible because we must assume both negligible erosion and negligible ^{10}Be losses to groundwater in the age calculations — assumptions that cannot be supported at the present time. Still, a rough time estimate is obtained by:

$$\Delta t = \frac{1}{\lambda} \times \ln \frac{R_{t1}}{R_{t2}} \quad (1)$$

where λ indicates a decay constant of ^{10}Be of 5×10^{-7} yr^{-1}, R_{t1} indicates the representative ($^{10}Be/^{9}Be_{reac}$) of timing of pedogenic calcrete formation and 3.37×10^{-9} is adopted. R_{t2} indicates the representative ($^{10}Be/^{9}Be_{reac}$) of timing of groundwater calcrete formation, and average ratio of the three calcrete samples of 1.28×10^{-9} is adopted for calculation. Then, the difference of timing formed groundwater and pedogenic calcrete calculates as 1.94 million years. We do not treat the ~2 million year age difference as necessarily precise or accurate. However, we do think it likely that somewhere on the order of a million years separated the formation of the groundwater calcrete and the pedogenic calcrete.

The integration of the Salt River across the Tempe Butte-Papago sill and its new course flowing into the Luke Basin (Figs. 2 and 4; Skotnicki and DePonty, 2020) likely initiated a knickzone that then

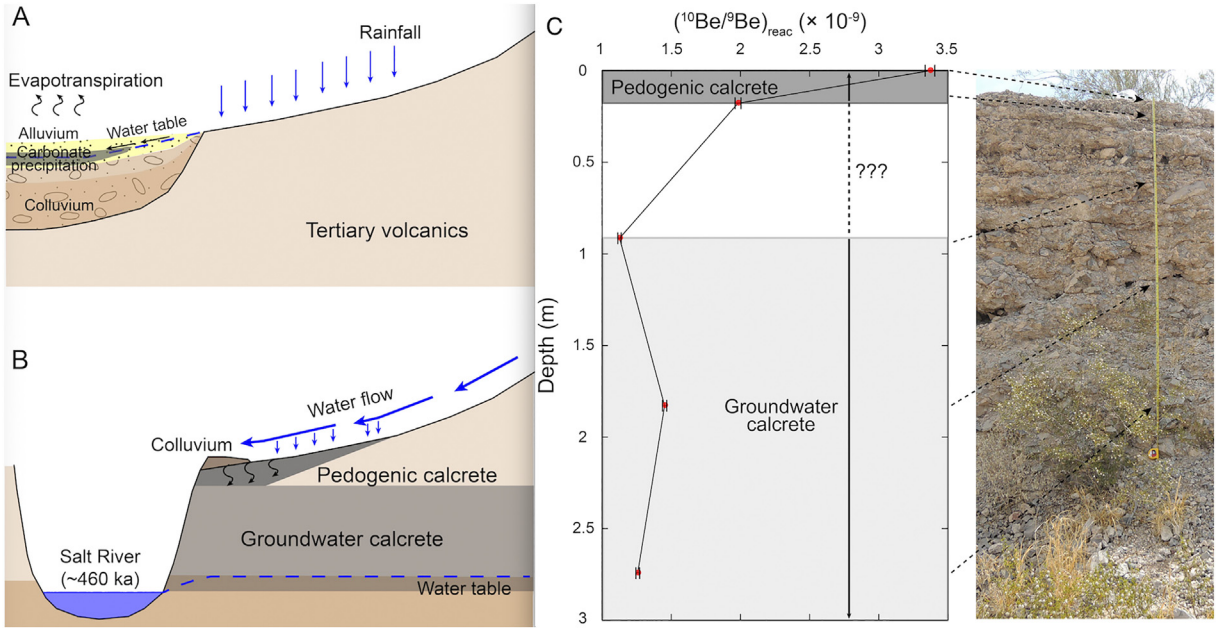

Fig. 10. Tempe Butte calcrete exposure interpreted using a meteoric $^{10}Be/^{9}Be_{reac}$ profile. A. Generalized profile of the western side of Tempe Butte showing conditions that allowed groundwater calcrete development when the ancestral Salt River gravels had aggraded to the point where they were at the elevation of the base of Tempe Butte. Abundant groundwater infused andesite colluvium with the calcrete. B. Dropping of the groundwater after the avulsion ca. 460 ka stopped any further development of groundwater calcrete. Subsequent calcrete development has been pedogenic. C. Plot of $^{10}Be/^{9}Be_{reac}$ samples versus depth, referenced with the photograph of the calcrete duricrust. The uppermost samples in the upper 0.2 m have a $^{10}Be/^{9}Be_{reac}$ signature indicating pedogenic formation, whereas the lower samples (0.9 m to 2.7 m depth) indicate groundwater formation. Because of the lack of samples from 0.2–0.9 m, we have no time information in the calcrete as indicated by the question marks.

migrated upstream leading to Salt River incision (Larson et al., 2020). This incision then likely dropped the water table and allowed development of pedogenic calcrete (Table 2). Thus, these meteoric ^{10}Be results are in general agreement with the time difference of ~2 million years between the arrival of the Salt River in this area and the transverse drainage development at the Tempe Butte-Papago sill that integrated the Higley and Luke basins in the Phoenix metropolitan area.

3.4. Spatial inequities in the source of Salt River deposits

When the natural lake within Tonto Basin first spilled over the sill near Roosevelt Dam, that discharge would have eroded the Mescal Limestone exposed immediately downstream (Scarborough, 1981; Spencer and Richard, 1999). This initial Salt River then carried Mescal Limestone (and other) fragments to at least the Stewart Mountain terrace (Dorn et al., 2020) where it mixed with locally derived alluvial-fan deposits of the Rolls formation. Then, as the knickpoint further excavated the sill at the site of Roosevelt Dam, the knickpoint would have propagated upstream and the excavation of Tonto Basin sediments would have been initiated.

The lithologic composition of the ASRD gravels, however, do not match the bedrock exposed in the bounding mountain ranges of the Tonto Basin: the steep Mazatzal Mountains on the west and the Sierra Ancha on the east of Tonto Basin. The Mazatzal bedrock feeding Tonto Basin is composed of coarse-grained granites, a large felsic hypabyssal intrusion, metabasalts and purple quartzite. The Sierra Ancha are underlain by coarse-grained granites and capped by the nearly flat-lying rocks of the Apache Group. Instead, the ASRD are dominated by clasts of dark gray argillite and quartzite (Skotnicki and DePonty, 2020).

Similarly, modern streams (and adjacent stream terraces) feeding sediment to the Salt River also do not match the ASRD. Purple quartzite dominates modern stream channels east of the northern Mazatzal Mountains, and Tonto Creek near Gisela, Arizona, contains mostly clasts of granophyre, granite, and ash-flow tuff. However, these clasts represent a very small percentage of the ASRD. Similarly, although red chert is ubiquitous in the Proterozoic formations in the northern Sierra Ancha and the northern Mazatzal Mountains, it too is quite rare in the ASRD.

The source of ASRD sediment and much of the materials in stream terraces and even the modern Salt River appear to derive from exposures of coarse rounded cobble deposits upstream and east of Tonto Basin. These have been interpreted (Faulds, 1986; Faulds, 1989; Potochnik, 1989) as early Tertiary sediments that were transported northeastward when southern Arizona was topographically higher than the modern Mogollon Rim. Faulds (1989) mapped the boundaries of these deposits and proposed that they filled a former wide river valley whose axis was approximately parallel with the modern river valley but flowed in the opposite direction, eastward. Nearly identical deposits mapped at the east end of modern-day Roosevelt Lake reservoir downdropped into Tonto Basin along the Meddler Wash fault (Skotnicki, 2003). Here, large rounded cobbles commonly exceeding 50 cm across form dissected basin-fill deposits that resemble the ASRD. Thus, we hypothesize that these older, early Tertiary deposits provided a substantial, but not yet quantified, amount of the sediment excavated by knickpoint retreat of the Salt River into the Tonto Basin and then subsequently deposited as the ASRD.

An independent assessment of the provenance of ASRD materials comes from detrital zircon (DZ) analyses (Dorn et al., 2020). Two depths of the BM well (Fig. 9) were sampled for DZ analyses, just above the cuttings with the 2.16 ± 0.48 Ma isochron burial age (ASRD) and just below the cuttings with the 3.90 ± 0.70 Ma isochron burial age (Rolls formation basin fill). The proposed excavation of the ASRD from early Tertiary Tonto Basin deposits would be consistent with a large peak in the DZ analyses near 1200 Ma that corresponds to published detrital zircon ages (Stewart et al., 2001) from the Dripping Spring Quartzite and from the Troy Quartzite.

4. Discussion

4.1. Drainage integration and reorganization of the Salt River system

The Salt and Verde rivers integrated after 3.3 Ma, based on deposition of Nomlaki tephra in lower Verde River Valley (LVRV) playa sediment (Dorn et al., 2020) and supported by a 3.9 ± 0.7 Ma isochron burial age (Fig. 8) from Rolls formation sediments underlying the ASRD in the Higley Basin. Because the LVRV (Figs. 2–6) is where these two rivers now meet, the Nomlaki tephra serves as a maximum limit for the timing of river integration. A paleomagnetic study (Bressler and Butler, 1978) in an upstream basin of the Verde River system, the Verde Valley (Fig. 2), indicates that lake sediments stopped depositing in that basin ca. 2.5 Ma. Soon after 2.5 Ma, a through-flowing Verde River was established and began incising (Pearthree, 1993) into basin fill in the Verde Valley.

The 2.5 Ma estimate for the initiation of the Verde River in the Verde Valley likely signals the initiation of a top-down sequence of basin integrating events (cf. Meek, 2020), similar to that on the lower Colorado River (e.g., Blackwelder, 1934; House et al., 2008), that ultimately leads to the arrival of the Verde River in the LVRV where it joins the Salt River. This 2.5 Ma estimate roughly matches our 2.2–2.8 Ma isochron cosmogenic burial ages for cuttings from two wells drilled into the ancestral Salt River deposits (ASRD) (Table 2; Figs. 8–9). These samples were not collected from near the base of the ASRD. Thus, 2.2 Ma and 2.8 Ma best represent minimum ages for the arrival of the Salt River in the Higley Basin at two different locations. The difference in these two isochron ages could be real, a reflection of different rates of deposition at different locations across this large basin (Fig. 2), or because of dating method uncertainties, or both.

Aggradation of the ASRD progressed in the Higley Basin from ca. 2.2–2.8 Ma until ca. 0.46 Ma. The 0.46 Ma age indicates the sudden arrival of the Salt River in the Luke Basin. Aggradation of the ASRD raised the Higley Basin's floor high enough to allow the Salt River to flow over the Tempe Butte-Papago sill at an elevation of approximately 326 m (1070 ft) (Skotnicki and DePonty, 2020). In the Luke Basin, the Salt River deposited ~30 m of gravel on top of endorheic basin fill deposits (Reynolds and Bartlett, 2002), marking this sudden arrival. The elevation of the Luke Basin just west of the airport was 293 m (Reynolds and Bartlett, 2002) and the elevation drop provided a steeper gradient than the Salt River east of the sill had at that time. In addition, by flowing westward into the Luke Basin instead of southward towards the location of the modern-day Gila River, the river length shortened by ~35 km. The combination of shortening and a significantly increased gradient must have led to incision of the Salt River, creating the Sawik stream terrace (named by Péwé, 1978) and abandoning the ASRD aggradational surface (Larson et al., 2020).

The timing of arrival of the Salt River into the Luke Basin ca. 0.46 Ma and the abandonment of ASRD is also consistent with a minimum ^{10}Be exposure age of ca. 333 ± 22 ka for the Sawik terrace collected from prior work (Seong et al., 2016a). Incision of the Salt River likely dropped the water table considerably, fitting the meteoric ^{10}Be analyses of calcrete present near the Tempe Butte-Papago sill presented in this study. The Salt River subsequently incised again at ~90 ka and then ~40 ka, producing the Mesa and Blue Point strath terraces, respectively (Larson et al., 2016; Larson et al., 2020). As Péwé (1978) originally observed, all three terraces are only found east of the location of aggradational piracy at the Tempe Butte-Papago bedrock sill; however, the reason for the incision that created these lower terraces is not known at present (Larson et al., 2020).

4.2. Determining the Salt, Verde, Gila sequence of arrival

We hypothesize that the Salt River and the Verde River integrated at about the same time, as indicated by a study of basalt outcrops where the Salt and Verde rivers would have first entered the LVRV (Dorn

et al., 2020). Trace element chemistry of whole rock basalt, major element chemistry of minerals, electron microscope back-scattered and cathodoluminescent textures, and strontium-isotope data all reveal matches between outcrop deposits and cobbles in the basal sediments of the ASRD. The matches occur in the lowest sampling intervals of drill cuttings extracted from two separate wells, but no such matches occurred in basalt gravels above the lower levels of the ASRD or beneath the ASRD in basin fill (Dorn et al., 2020). The reason for the lack of matches above the lower levels of the ASRD is that the Salt and Verde rivers only eroded the outcrop positions of the basalt when they first arrived.

The rough similarity in the timing of Verde River and Salt River integration ca. 2.2–2.8 Ma (Table 2; Bressler and Butler, 1978), along with Verde- and Salt-sourced basalt gravels in the same basal ASRD sampling interval in cuttings extracted from two separate wells (Dorn et al., 2020), raises the question of whether the Gila River's integration occurred before, after, or at about the same time as the Verde and Salt rivers. Jungers and Heimsath (2016) indicate that Gila River deposits arrived in the Safford Basin ~2.8–3 Ma and that deep basin incision had occurred after about 2.0 Ma, but nothing direct can be inferred from their research about the Gila River's integration in the Phoenix area. In a detailed analysis of the Gila River's integration, Gootee et al. (2020) are not able to determine a precise age for when Gila River arrived in the modern-day Phoenix valley, but they suspect its integration may have come after the Salt and Verde rivers. It is possible, also, that all of the exoreic streams of central Arizona formed at about the same time.

Certainly, it is extremely unlikely that an overfill condition developed in the various basins of the Gila, Verde, and Salt at the same time in the absence of external forcing. However, the extensional basins in central Arizona could have hosted lakes that overflowed in a particularly wet climatic period, as has been suggested by others for the Colorado and Rio Grande (Chapin, 2008; Repasch et al., 2017). Unfortunately, current dating results have neither the precision nor the accuracy to address the sequence of central Arizona river integration. Even the ~3 m sampling interval where Verde and Salt basalt clasts co-occur could have aggraded in the ASRD over a time interval of 10^3–10^4 yr.

Identifying unique Gila, Verde, and Salt clasts in other well cuttings could assist in evaluating this question, as would identifying source-specific rocks in deposits in the lower Gila River associated with Sentinal volcanics, such as finding Verde-derived basalts (Dorn et al., 2020) underneath a Sentinal ca. 2.3 Ma basalt flow (Cave and Greeley, 2004; Cave, 2015). The first author examined cuttings from City of Goodyear Well 24 and recorded deposits with a composition that could reflect either Gila- or Salt-sourced sediment at an elevation of 282 m (925 ft). This sediment rests directly on playa deposits of the Luke Basin and likely reflects the first arrival of exoreic water into that basin. Thus, with further research on the age and provenance of this sort of first-arrived sample, it may be possible determine whether the Salt and Verde rivers or the Gila River integrated first. However, the geomorphology of the LVRV offers some insight about the order of Salt and Verde integration.

The presence of the Mescal limestone on the strath Stewart Mountain terrace (SMT) (Dorn et al., 2020) would be difficult to explain if the Verde River integrated first. A channel incised into the Pemberton playa in the LVRV led to a drop in the local base level of ephemeral streams from the nearby McDowell Mountain pediment, and these streams truncated playa sediment — followed soon after by aggradation of Lousley Hills gravels on top of this truncated surface (Larson et al., 2020) starting about 2.2 Ma (Fig. 7; Table 2). A channel cut into the Pemberton playa sediment would have required that the Rolls formation alluvial-fan ramp had already undergone incision near the present-day position of Granite Reef (Fig. 4). If the Verde River arrived first and started incising into the Rolls formation, then the Mescal limestone would not have been deposited on the SMT.

A newly arrived Salt River flowing on the Rolls formation alluvial fan would have encountered a knickpoint at its new junction with an incised Verde River. The recession of this knickpoint back through the Rolls formation would not have allowed time for mixing of Mescal limestone limestone with Rolls formation materials. The Salt River would have likely been a series of retreating rapids (knickzones) and the position of the SMT would have been too high to allow Mescal limestone integration into the upper Rolls formation.

The reason is that the position of the SMT strath cut into the Rolls formation would have been too high above a Salt River. The only remaining explanation for the Mescal limestone's presence on the SMT is that the Salt arrived first, mixed Salt gravels (e.g., Mescal limestone) with Rolls formation materials and then abandoned the strath SMT with further incision. Then, a later-arriving Verde River would have had a ready-made knickpoint when it flowed over the SMT down towards lower Salt River. This knickpoint would have retreated, leading to the observed channel cut into the Pemberton playa.

4.3. Overfill of basins in extensional settings

Overfill of basins in extensional tectonic contexts are widely recognized (Flemings and Jordan, 1989; Catuneanu, 2004; Dickinson, 2015; McGlue et al., 2016). Thus, an overfill condition occurring between the lower Verde River valley (LVRV) and the Higley Basin (Figs. 2–5) should not be a surprise. However, we are not aware of another case where overspill has been documented through connecting deposits recognized at the surface in the upstream basin (LVRV) and in wells cuttings in the downstream basin (Higley) (Figs. 2–5). The distinctive fanglomerate of the Rolls formation (Rf) exists as preserved exposures in the LVRV. Large meter-sized clasts of the Rf, likely carried by debris flows, aided its geomorphic preservation at the SMT and the Rolls. This alluvial-fan ramp transported Rf (Fig. 5) sediment for at least the latter half of the Pliocene, indicated by an isochron burial age near the top of the Rf at 3.9 ± 0.7 Ma (Table 2 and Fig. 8). When the Salt and Verde rivers arrived into the LVRV sometime around 2.2–2.8 Ma (Table 2), the rivers used this fan ramp to transport largely boulders and gravels into the Higley Basin. These ancestral Salt River deposits aggraded directly on top of the underlying Rolls formation materials, as recorded in well cuttings (Skotnicki and DePonty, 2020).

Fig. 11 summarizes the development of the Salt River upon its departure from the LVRV on the fan ramp and its entrance into the supradetachment extensional setting of the Phoenix metropolitan area. The cross section in Fig. 11 runs down the ASRD (Figs. 2 and 3B) from the entrance of the Salt River at the Granite Reef bedrock sill southward towards the limit of ASRD sampling near its probable junction with the Gila River (Skotnicki and DePonty, 2020). The pre-Salt River gradient measures at about 6 m/km based on an analysis of well cuttings (Skotnicki and DePonty, 2020). As the ASRD aggraded, the slope lessened to about 4 m/km at its top.

4.4. No tectonic signature in the Salt River stream terraces

Péwé (1978) originally observed an upstream topographic divergence in the longitudinal profiles of the Salt River stream terraces, where the oldest and highest Sawik terrace tread had the steepest longitudinal profile and the lower Mesa, Blue Point, and Lehi terrace treads had progressively lower gradients. Péwé (1978) interpreted this progressive decrease in longitudinal profile gradient over time as a reflection of neotectonic uplift of the Mogollon Rim. Larson et al. (2010) offered up another possibility: that gradual enlargement of the Salt River drainage area upon integration of the Salt River near Roosevelt Dam (R, Fig. 4) would produce this same pattern over time. Although both hypotheses were reasonable at the time, the reality of exactly what happened to produce the Salt River's stream terraces speak to the importance of very different basin integration processes that created

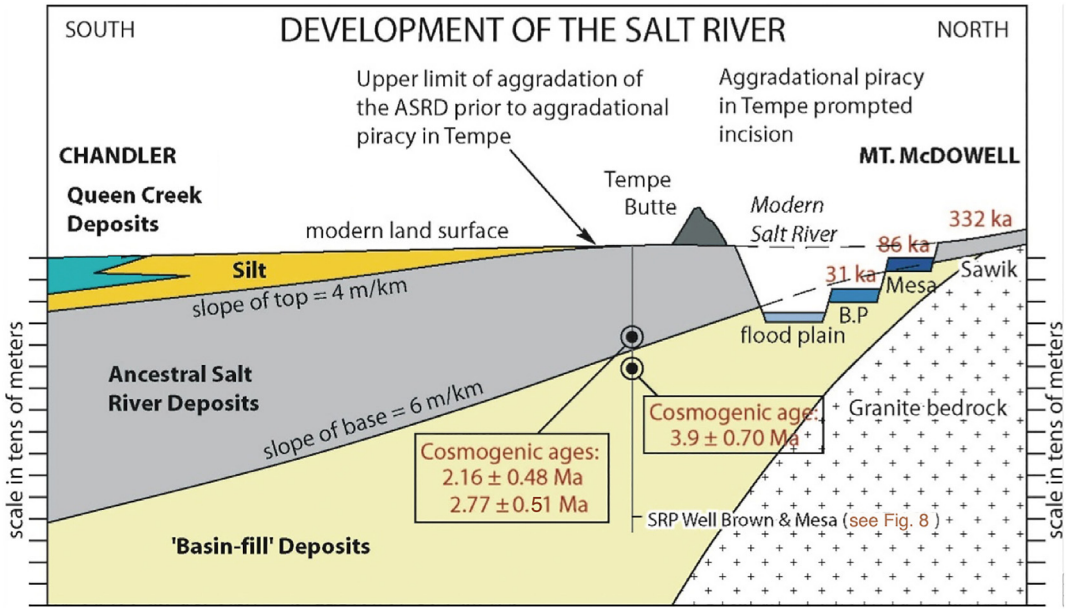

Fig. 11. Development of the Salt River in the Higley Basin that underlies the eastern part of metropolitan Phoenix in an idealized cross section from the entrance point at Granite Reef Dam to the limit of our ASRD mapping (Skotnicki and DePonty, 2020). The "basin fill" is the term widely used to indicate closed-basin deposits throughout the Basin and Range Province. Here, we recognize these as being the Rolls formation with an isochron burial age of ca. 3.9 Ma near the top of the deposit. Upon drainage integration sometime between 2.2 and 2.8 Ma, the Salt River flowed onto the top of the basin fill (Rolls formation) and proceeded to aggrade about 30–40 m of gravels over the next ca. 2 million yr. Then, around 460 ka, an avulsion occurred via aggradational piracy (or aggradational spillover via fluvial aggradation; Hilgendorft et al., 2020) near Tempe Butte, leading to incision of the Salt River channel upstream, east of this avulsion. This incision was followed by upstream river terrace formation.

transverse drainage sections of the Salt River and produced these stream terraces

The highest Salt River terrace, Stewart Mountain terrace (SMT), was identified by Larson et al. (2010). We interpret SMT here as a strath terrace cut in the surface of the Rolls formation alluvial fan (Fig. 5). At present, absolute age control for SMT has been difficult to obtain and efforts are ongoing. However, given its topographic position, stratigraphic relationships, and sedimentological characteristics, we can support the conclusion of the SMT as the oldest Salt River terrace. We hypothesize that the SMT resulted from overflow processes that integrated the Tonto Basin with the lower Verde Basin near the modern-day location of Roosevelt Dam (Figs. 2–4). Mescal limestone is present at the surface of the SMT, but has not yet been found in the Rolls formation (Dorn et al., 2020). The only outcrops of the Mescal limestone in reasonable proximity to SMT are found near the modern-day Roosevelt Dam. Our current interpretation is that Mescal limestone clasts were transported to the SMT as the overflow-generated knickpoint migrated headward into the Tonto Basin. These clasts were mixed with Rolls formation fanglomerate on top of the SMT as the Salt River flowed across it. We interpret the SMT morphology observed today as primarily a product of this eroded Rolls formation alluvial fan surface and degradation of this surface through time since it was abandoned by the Salt River. As such, the longitudinal profile of the SMT surface and its high topographic position above the modern-day Salt River should not be used to infer and does not require uplift of the Mogollon Rim during the Quaternary to explain its gradient.

Péwé's (1978) Sawik terrace is the next highest and second oldest terrace of the Salt River. The Sawik terrace has a minimum ^{10}Be exposure age of ca. 333 ± 22 ka (Seong et al., 2016a). Skotnicki and DePonty (2020) and Larson et al. (2020) interpret the Sawik terrace tread and its longitudinal profile as the highest elevation of aggradation of the ASRD within the Higley Basin (Skotnicki and DePonty, 2020). Buried gravels resting on top of an eroded granitic pediment indicate a flowing river was at the elevation of this terrace ca. 692 ± 35 ka (Seong et al., 2016a). This surface was then abandoned following aggradational spillover of the Salt River from the Higley Basin into the Luke Basin ca. 460 ka. This led to retreat of a knickpoint and headward wave of incision that abandoned the ASRD surface in the Higley Basin and formed the Sawik terrace (Larson et al., 2020).

Although it is possible that the Mesa (~90 ka; Larson et al., 2016) and Blue Point (~36 ka; Larson et al., 2016) terraces' topographic divergence could be in response to tectonism that occurred in the last 100,000 yr — there is no evidence of any significant late Quaternary faulting in the region that could have produced the different longitudinal profiles that Péwé (1978) observed. We can only speculate that climatically driven change in sediment supply and discharge may have resulted in incision and formation of these terraces – as well as the observed differences in longitudinal profile gradients. Given the basin-wide geomorphic relationships between a variety of landforms and the slope of the Mesa terrace, it seems clear that the Mesa terrace tread represents approximately a quarter million years of relative stability in the longitudinal profile and drainage basin of the Salt River following knick-recession and adjustment to abandonment of the Sawik terrace surface (Larson et al., 2016; Larson et al., 2020).

4.5. Broader context of the Salt River's integration

In developing a better understanding of drainage integration in the extensional tectonic setting of the Basin and Range Province (BRP) of western North America, Norman Meek laid the foundation for the importance of sediment reducing the volume of endorheic basins, followed by lake overflow during a particularly wet climatic interval (Meek, 1989, 2004, 2020). Meek's dissertation research on extension of major streams from the top down was later replicated and expanded for the Mojave River and Afton Canyon area (Reheis et al., 2007; Reheis and Edwine, 2008). In the decades following Meek's research, lake overflow has become recognized widely as a key process of drainage integration along the lower Colorado and Rio Grande rivers (Spencer and Pearthree, 2001; House et al., 2008; Roskowski et al., 2010; Spencer, 2011a; Repasch et al., 2017). Both the lower Colorado and Rio Grande, however, integrated along rift tectonic settings (Friedmann and

Burbank, 1995), albeit with major structural and topographic barriers still in the way.

The original model for drainage prolongation by lake overflow (Meek, 1989; Meek, 2020), where Lake Manix overflowed through Afton Canyon in the Mojave Desert, is not now in a tectonic rift extensional continental setting — although extension dominated in the Miocene. At present, the Afton Canyon region exists in a larger shear zone dominated by strike-slip faulting with some extension (Savage et al., 1990; Nuriel et al., 2019).

In contrast, the Salt and Verde rivers integrated ca. 2.2–2.8 Ma across still different extensional tectonic settings. The Salt and the Verde rivers both began river integration by getting across fault-block mountains in the upper portions of their watersheds; this was accomplished by Meek's (1989, 2020) process of volume reduction by sedimentary infilling, followed by lake overflow. After lake overflow, both rivers entered a tectonic setting of the half-graben lower Verde River valley (LVRV) that had already reached a condition of overfill. Although basin overfilling is recognized as an important process of drainage integration in numerical modeling studies (Geurts et al., 2018; Geurts et al., 2020), the idea of a newly integrated river system flowing on an alluvial-fan ramp is different from previous BRP river integration research.

We view the Salt and Verde watershed integration as further illustration that a "top down" model occurs in a variety of extensional tectonic frameworks. The lower Colorado River (House et al., 2008; Spencer, 2011a; Howard et al., 2015) and Rio Grande (Connell et al., 2005; Repasch et al., 2017) integrated in a top-down fashion. The Salt and Verde rivers integrated across rift half-grabens and then across a supradetachment extensional setting, where the sequence portrayed in Fig. 11 is just east of the South Mountains metamorphic core complex (Reynolds, 1985; Spencer and Reynolds, 1989; Reynolds and Lister, 1990; Livaccari et al., 1995).

This case study of the Salt and Verde rivers also offers insight into the power of outcrop geology in understanding drainage integration. Because the first author participated in the geological mapping of quadrangles throughout the study region (Skotnicki and Ferguson, 1995; Ferguson and Skotnicki, 1996; Skotnicki, 1996; Skotnicki and Leighty, 1997; Ferguson et al., 1998; Skotnicki and Leighty, 1998; Skotnicki, 2000; Skotnicki, 2003), he recognized that the Salt River gravels extracted from the well cuttings (Skotnicki and DePonty, 2020) and observed in stream terrace and modern stream gravels do not have a close match with potential bedrock sources upstream. Certainly, bedrock from drainage basin sources contributed, but not dominantly. Instead, gravels in the Salt River system including the ASRD appear to derive from a different source, very possibly from Tertiary alluvium within the Tonto Basin that were once trying to reach base level in northeastward flowing drainages (Faulds, 1986; Faulds, 1989; Potochnik, 1989). These gravel deposits eroded as a result of knickpoint recession after lake overflow near modern day Roosevelt Dam, and were transported to the southwest by the newly formed Salt River system.

5. Conclusion

The Salt and Verde rivers did not exist as through-flowing streams until after 3.3 Ma, as indicated by deposition of Nomlaki tuff in closed-basin deposits of the lower Verde River valley (LVRV) near the junction of these rivers. In his last paper, type set after his death, W.M. Davis' (1933, p. 8) described the first key process in the many steps leading to today's integrated drainage:

> "The ranges appear to have originated as diversely displaced fault blocks, like those of Arizona ... it is highly probable that their initial intermont troughs were for a time without discharge to the sea... Under such conditions the basins would be aggraded with waste downwashed from the mountains... Each trough floor would thus be built up to higher and higher levels, and in time and outflow might be established at the lowest sag of the enclosing mountains: for just there the least in-wash of detritus would be received, and the trough-floor playa would therefore be pushed towards the sag until overflow resulted..."

For much of the Pliocene, the Rolls formation fanglomerate accumulated in the axial drainage of the LVRV. Then, when the LVRV filled up completely, an alluvial-fan ramp crossed into the next lower, Higley closed basin, transporting the Rolls formation via ephemeral flow.

The first discharge of the Salt River probably resulted from lake overflow from the Tonto Basin near the present-day position of Roosevelt Dam. The overflow could have occurred before 2.8 Ma, the oldest burial age for Salt River gravels deposited into the Higley Basin, but definitely by 2.2 Ma. Mescal limestone gravels, with the only known upstream source being near Roosevelt Dam, were eroded and then transported by the Salt River that flowed in the low spot occupied by the Rolls formation axial fan system. Again, W.M. Davis (1933, p. 9) explained what might have happened next:

> "After a basin outlet was developed, it would be rapidly cut down in a steep-walled gorge; the detritus of the aggraded basin should be as actively eroded by an axial stream, which might well maintain a graded course to the deepening outlet gorge…"

The Rolls formation alluvial-fan ramp had a slope at the time of Salt River arrival of 6 m/km. This type of a slope is typical for an alluvial fan, but a river should do what W.M. Davis (1933) indicated: incise an outlet gorge just downstream of present-day Granite Reef Dam.

We speculate that the resulting knickzone would have worked back upstream, eroding into the Rolls formation and abandoning its initial floodplain. This process, thus, resulted in the Stewart Mountain terrace (SMT): a strath terrace cut into the Rolls formation with mixed-in clasts of river-transported sediment such as the Mescal limestone. The Salt River would have then continued to incise into the Rolls formation, all while its bedload was deposited as the ancestral Salt River deposits (ASRD) in the Higley Basin, as well as most of the bedload transported downstream.

A large lake of the Verde Valley deposited its last bit of limestone about 2.5 Ma, at which time the Verde River came into existence — filling and then spilling over Horseshoe and Bartlett basins, before entering the LVRV. We hypothesize that the arrival of the Verde River in the LVRV was through the process of lake overflow that occurred somewhere near modern-day Bartlett Dam. The Verde River's arrival took place very near in time to the arrival of the Salt River, as indicated by basalt clasts in well cuttings sourced to outcrops where both rivers would have entered the LVRV. The sourced basalt clasts are found near the basal deposits of the ASRD in two different wells.

We suspect the Salt River was the first of central Arizona's exoreic rivers, because a knickpoint appears to have worked headward from the modern-day Salt-Verde junction up through the adjacent Pemberton playa. This knickpoint's existence is known through playa deposits that were truncated by local (McDowell Mountain) tributary streams, where the truncated surface had a gradient flowing towards the Verde River's location of about a meter per kilometer. A reasonable way this knickpoint could have formed is by the newly-arrived waters of the Verde River.

Verde River waters would have quickly spread out over the Pemberton playa's surface, and then focused to flow across the SMT at the present-day location of the Salt-Verde junction. These waters would have then experienced a waterfall as they flowed down the side of the SMT towards the incised Salt River. A knickpoint would have quickly retreated headward through the SMT and then cut the known channel into the Pemberton playa.

The lake spillover event near Bartlett Dam would have also done what Davis (1933, p. 10) described: "it would be rapidly cut down in a

steep-walled gorge" and then excavated the old basin fill from Bartlett and Horseshoe basins. This fill material would not have been rounded, consisting of alluvial-fan deposits. Concomitantly, such materials are found burying the truncated playa surface immediately downstream from Bartlett Dam in the form of the Lousley Hills gravels, where the base of these gravels resting on the truncated playa surface have a burial age of 2.2 Ma.

These initial exoreic waters then entered the Higley Basin underlying today's eastern metropolitan Phoenix, USA, by flowing on an alluvial-fan ramp. For about 2 million years, the integrated river deposited gravels across a wide floodplain that could be called a megafan. Aggradation of these gravels reduced gradient of this floodplain from 6 m/km at the start to 4 m/km by about 460 ka, at which time an avulsion took place across a low spot in a bedrock ridge that separates the Higley Basin from the Luke Basin. Through the process of aggradational piracy (or aggradational spillover via fluvial aggradation), the Salt River's channel shortened by ~35 km and suddenly deposited 30 m of gravels west of the avulsion location. Salt River incision then ensued east of the avulsion, dropping the water table and leading to the formation of a stream terrace.

Meek (1989, 2020) proposed a general framework of drainage integration in the Basin and Range extensional tectonic terrain that involves regional prolongation of rivers through lake overflow, a model later replicated for his tectonically extended and then sheared study area of Lake Manix and Afton Canyon in the Mojave Desert (Reheis et al., 2007; Reheis and Edwine, 2008). A top-down model of regional drainage prolongation is consistent with evidence along the lower Colorado and Rio Grande rivers (Spencer and Pearthree, 2001; Connell et al., 2005; Roskowski et al., 2010; Spencer, 2011a; Repasch et al., 2017) in a rift tectonic setting (Friedmann and Burbank, 1995). The Salt and Verde rivers also integrated in a top-down fashion through a combination of sediment infilling of basins and lake overflow across fault-block mountains and a supradetachment extensional setting. Top-down river integration via sediment infilling of endorheic basins followed by lake overflow appears to explain the development of all of the exoreic rivers that occur in the extensional Basin and Range Province of western North America.

Declaration of competing interest

The authors declare that they have no known competing financial interests or personal relationships that could have appeared to influence the work reported in this paper.

Acknowledgements

We thank three reviewers for their suggestions, Doug Bartlett for providing access to Salt River gravel samples from the aggradational piracy event, the Salt River Project and a Minnesota State Faculty Research Grant for financial support, and Ariel Shamas for help in designing the artistic portrayal of the Pliocene lower Verde River valley.

Appendix A. Supplementary data

Supplementary data associated with this article can be found in the online version, at https://doi.org/10.1016/j.geomorph.2020.107512. These data include the Google map of the most important areas described in this article.

References

Anderson, L.W., Piety, L.A., 1987. Surficial Geologic Map of the Tonto Basin. U.S. Bureau of Reclamation, Denver (1 sheet, scale 1:48,000).

Anderson, L., Piety, L.A. (Eds.), 1988. Field-Trip Guidebook to the Tonto Basin: Geomorphology, Quaternary Geology, Tertiary Basin Development, Archaeology, and Engineering Geology: Friends of the Pleistocene (Rocky Mountain Cell of the Friends of the Pleistocene).

Balco, G., Rovey, C.W., 2008. An isochron method for cosmogenic-nuclide dating of buried soils and sediments. Am. J. Sci. 308, 1083–1114.

Balco, G., Stone, J., Jennings, C., 2005. Dating Plio-Pleistocene glacial sediments using the cosmic-ray-produced radionuclides 10Be and 26Al. Am. J. Sci. 305, 1–41.

Balco, G., Stone, J.O., Lifton, N.A., Dunai, T.J., 2008. A complete and easily accessible means of calculating surface exposure ages or erosion rates from 10 Be and 26 Al measurements. Quat. Geochronol. 3, 174–195.

Bishop, P., 1995. Drainage rearrangement by river capture, beheading and diversion. Prog. Phys. Geogr. 19, 449–473.

Blackwelder, E., 1934. Origin of the Colorado River. Bull. Geol. Soc. Am. 45, 551–566.

Bostwick, T.W., 2002. Landscape of the Spirits: Hohokam Rock Art at South Mountain Park. University of Arizona Press, Tucson.

Bourlès, D., Raisbeck, G.M., Yiou, F., 1989. 10Be and 9Be in marine sediments and their potential for dating. Geochim. Cosmochim. Acta 53, 443–452.

Bressler, S.L., Butler, R.F., 1978. Magnetostratigraphy of the late Tertiary Verde Formation, central Arizona. Earth Planet. Sci. Lett. 38, 319–330.

Burchfiel, B.C., Nakov, R., Dumurdzanov, N., Papanikolaou, D., Tzankov, T., Serafimovski, T., King, R.W., Kotzev, V., Todosov, A., Nurce, B., 2008. Evolution and dynamics of the Cenozoic tectonics of the South Balkan extensional system. Geosphere 4, 919–993.

Catuneanu, O., 2004. Retroarc foreland systems––evolution through time. J. Afr. Earth Sci. 38, 225–242.

Cave, S.R., 2015. The Sentinel-Arlington Volcanic Field, Arizona. Ph.D. Dissertation. Arizona State University, Tempe (59).

Cave, S., Greeley, R., 2004. The geology of two small Cenozoic Volcanoes in Southwestern Arizona. J. Ariz. Nev. Acad. Sci. 37, 105–110.

Chapin, C.E., 2008. Interplay of oceanographic and paleoclimate events with tectonism during middle to late Miocene sedimentation across the southwestern USA. Geosphere 4, 976–991.

Chapman, A.D., Rautela, O., Shields, J., Ducea, M.N., Saleeby, J., 2019. Fate of the lower lithosphere during shallow-angle subduction; the Laramide example. GSA Today 30. https://www.geosociety.org/gsatoday/science/G412A/article.htm.

Chmeleff, J., von Blanckenburg, F., Kossert, K., Jakob, D., 2010. Determination of the 10 Be half-life by multicollector ICP-MS and liquid scintillation counting. Nucl. Instrum. Methods Phys. Res., Sect. B 268, 192–199.

Connell, S.D., Hawley, J.W., Love, D.W., 2005. Late Cenozoic drainage development in the southeastern Basin and Range of New Mexico, Southeasternmost Arizona, and western Texas. New Mexico Museum of Natural History and Science Bulletin 28, 125–150.

Davis, W.M., 1933. Geomorphology of mountainous deserts. Balsch Graduate School of the Geological Sciences California Institute of Technology Contribution 188, 1–12.

Dickinson, W.R., 2015. Integration of the Gila River drainage system through the Basin and Range province of southern Arizona and southwestern New Mexico (USA). Geomorphology 236, 1–24.

Dorn, R.I., Skotnicki, S.J., Wittman, A., Van Soest, M., 2020. Provenance in drainage integration research: Case studies from the Phoenix metropolitan area, south-central Arizona. Geomorphology 369. https://www.sciencedirect.com/science/article/pii/S0169555X20304037.

Douglass, J., Schmeeckle, M.W., 2007. Analogue modeling of transverse drainage mechanisms. Geomorphology 84, 22–43.

Douglass, J., Meek, N., Dorn, R.I., Schmeeckle, M.W., 2009a. A criteria-based methodology for determining the mechanism of transverse drainage development, with application to southwestern USA. Geol. Soc. Am. Bull. 121, 586–598.

Douglass, J., Meek, N., Dorn, R.I., Schmeeckle, M.W., 2009b. Data Repository for GSA Bulletin Submission 2007: a criteria-based methodology for determining the mechanism of transverse drainage development, with application to southwestern USA. Geological Society of America Bulletin Data Repository ftp://rock.geosociety.org/pub/reposit/2008/2008163.pdf.

Eaton, G.P., 1982. The Basin and Range province: origin and tectonic significance. Annu. Rev. Earth Planet. Sci. 10, 409–440.

Erlanger, E.D., Granger, D.E., Gibbon, R.J., 2012. Rock uplift rates in South Africa from isochron burial dating of fluvial and marine terraces. Geology 40, 1019–1022.

Faulds, J.E., 1986. Tertiary Geologic History of the Salt River Canyon Region, Gila County, Arizona. University of Arizona, M.A. Thesis, pp. 1–334.

Faulds, J.E., 1989. Geologic map of the Salt River Region, Rockinstraw Mountain Quadrangle, Gila County, Arizona. Arizona Geological Survey Contributed Map CM-89-B (map scale 1:24,000, 003 map sheets).

Ferguson, C.A., Skotnicki, S.J., 1996. Bedrock geology of the Santan Mountains, Pinal and Maricopa Counties, Arizona. Arizona Geological Survey Open File Report OFR-96-09, pp. 1–22.

Ferguson, C.A., Skotnicki, S.J., Gilbert, W.G., 1998. Geologic map of the Tonto Basin 7.5′ quadrangle, Gila and Maricopa Counties, Arizona. Arizona Geological Survey Open-File Report 98-16, 1–15.

Flemings, P.B., Jordan, T.E., 1989. A synthetic stratigraphic model of foreland basin development. Journal of Geophysical Research: Solid Earth 94, 3851–3866.

Friedmann, S.J., Burbank, D.W., 1995. Rift basins and supradetachment basins: Intracontinental extensional end-members. Basin Res. 7, 109–127.

Geurts, A.H., Cowie, P.A., Duclaux, G., Gawthorpe, R.L., Huismans, R.S., Pedersen, V.K., Wedmore, L.N., 2018. Drainage integration and sediment dispersal in active continental rifts: a numerical modelling study of the central Italian Apennines. Basin Res. 30, 965–989.

Geurts, A.H., Whittaker, A.C., Gawthorpe, R.L., Cowie, P.A., 2020. Transient landscape and stratigraphic responses to drainage integration in the actively extending central Italian Apennines. Geomorphology 369. https://www-sciencedirect-com/science/article/pii/S0169555X19305045.

Gootee, B.F., 2013. An evaluation of carbon dioxide sequestration potential in the higley Basin, South-Central Arizona. Arizona Geological Survey Open File Report, OFR-13-10 (14 p., 6 map plates and 2 appendices).

Gootee, B.F., Skotnicki, S.J., Seong, Y.B., 2020. Plio-Pleistocene Stability of the Queen Creek Drainage in the Basin and Range Province, Eastern Phoenix Metropolitan Area, Central Arizona. Geomorphology (This issue).

Granger, D.E., Muzikar, P.F., 2001. Dating sediment burial with in situ-produced cosmogenic nuclides: theory, techniques, and limitations. Earth and Planetary Science Letters 269–281.

Hildabrand, T.C., 2015. Lithofacies Characterization and Chemostratigraphy of the Pliocene Verde Formation, Northern Verde Valley, Central Arizona. Northern Arizona University, M.S. Thesis, pp. 1–143.

Hilgendorft, Z., Wells, G., Larson, P.H., Millett, J.J.F., Kohout, M.A., 2020. From basins to rivers: Understanding the revitalization and significance of top-down drainage integration mechanisms in drainage basin evolution. Geomorphology 369. https://doi.org/10.1016/j.geomorph.2019.107020.

House, P.K., Pearthree, P.A., Perkins, M.E., 2008. Stratigraphic evidence for the role of lake spillover in the inception of the lower Colorado River in southern Nevada and western Arizona. Geol. Soc. Am. Spec. Pap. 439, 335–353. https://doi.org/10.1130/2008.2439(15).

Howard, K.A., House, P.K., Dorsey, R.J., Pearthree, P.A., 2015. River-evolution and tectonic implications of a major Pliocene aggradation on the lower Colorado River: the Bullhead Alluvium. Geosphere 11, 1–30.

Jeong, A., Lee, J.I., Seong, Y.B., Balco, G., Yoo, K.-C., Yoon, H.I., Domack, E., Rhee, H.H., Yu, B. Y., 2018. Late Quaternary deglacial history across the Larsen B embayment, Antarctica. Quat. Sci. Rev. 189, 134–148.

Jungers, M.C., Heimsath, A.M., 2016. Post-tectonic landscape evolution of a coupled basin and range: Pinaleño Mountains and Safford Basin, southeastern Arizona. Geol. Soc. Am. Bull. 128 (469–486).

Kohl, C.P., Nishiizumi, K., 1992. Chemical isolation of quartz for measurement of in-situ-produced cosmogenic nuclides. Geochim. Cosmochim. Acta 56, 3583–3587.

Korschinek, G., Bergmaier, A., Faestermann, T., Gerstmann, U.C., Knie, K., Rugel, G., Wallner, A., Dillmann, I., Dollinger, G., Lierse von Gostomski, C., Kossert, K., Maiti, M., M., P, Remmert, A., 2010. A new value for the half-life of 10 Be by heavy-ion elastic recoil detection and liquid scintillation counting. Nucl. Instrum. Methods Phys. Res., Sect. B 268, 187–191.

Lance, J.F., Downey, J.S., Alford, M., 1962. Cenozoic sedimentary rocks of the Tonto Basin. In: Weber, R.H., Peirce, W.H. (Eds.), Mogollon Rim Region (East-Central Arizona). New Mexico Geological Society 13th Annual Fall Field Conference Guidebook. New Mexico Geological Society, Socorro, pp. 98–99.

Laney, R.L., Hahn, M.E., 1986. Hydrogeology of the eastern part of the Salt River Valley area, Maricopa and Pinal Counties, Arizona. U.S. Geological Survey Water-Resources Investigations Report 86-4147 (4 plates).

Larson, P.H., Dorn, R.I., Douglass, J., Gootee, B.F., Arrowsmith, R., 2010. Stewart Mountain Terrace: a new Salt River terrace with implications for landscape evolution of the lower Salt River Valley, Arizona. J. Ariz. Nev. Acad. Sci. 42, 26–36.

Larson, P.H., Dorn, R.I., Palmer, R.E., Bowles, Z., Harrison, E., Kelley, S., Schmeeckle, M.W., Douglass, J., 2014. Pediment response to drainage basin evolution in south-central Arizona. Phys. Geogr. 35, 369–389.

Larson, P.H., Kelley, S.B., Dorn, R.I., Seong, Y.B., 2016. Pace of landscape change and pediment development in the northeastern Sonoran Desert, United States. Ann. Assoc. Am. Geogr. 106, 1195–1216.

Larson, P.H., Meek, N., Douglass, J.C., Dorn, R.I., Seong, Y.B., 2017. How rivers get across mountains: a new landscape via transverse drainage. Ann. Assoc. Am. Geogr. 107, 274–283.

Larson, P.H., Dorn, R.I., Skotnicki, S., Yeong, S.B., Jeong, A., 2020. Impact of drainage integration on basin geomorphology and landform evolution: case study along the Salt and Verde Rivers, Sonoran Desert. USA. Geomorphology 369. https://doi.org/10.1016/j.geomorph.2020.107439.

Leighty, R.S., Skotnicki, S.J., Pearthree, P.A., 1997. Geologic map of the Cave Creek Quadrangle, Maricopa County, Arizona. Arizona Geological Survey Open File Report, OFR-97-01 (2 map sheets, map scales 1:24,000 and 1:12,000, 38).

Livaccari, R.F., Geissman, J.W., Reynolds, S.J., 1995. Large-magnitude extensional deformation in the South Mountains metamorphic core complex, Arizona. Geol. Soc. Am. Bull. 107, 877–894.

McGlue, M.M., Smith, P.H., Zani, H., Silva, A., Carrapa, B., Cohen, A.S., Pepper, M.B., 2016. An integrated sedimentary systems analysis of the Rio Bermejo (Argentina): Megafan character in the overfilled southern Chaco Foreland basin. J. Sediment. Res. 86, 1359–1377.

Meek, N., 1989. Geomorphic and hydrologic implications of the rapid incision of Afton Canyon, Mojave Desert, California. Geology 17, 7–10.

Meek, N., 2004. Mojave River history from an upstream perspective. In: Reynolds, R.E. (Ed.), Breaking Up — the 2004 Desert Symposium Field Trip and Abstracts. California State University Fullerton Desert Studies Consortium, Fullerton, CA., pp. 41–49

Meek, N., 2020. Episodic forward prolongation of trunk channels in the western USA. Geomorphology, this issue https://doi.org/10.1016/j.geomorph.2019.05.002.

Menges, C.M., Pearthree, P.A., 1983. Map of Neotectonic (Latest Pliocene-Quaternary) Deformation in Arizona. Arizona Geological Survey Open File Report, OFR-83-22 (3 map sheet, map scale 1:500,000).

Nuriel, P., Miller, D.M., Schmidt, K.M., Coble, M.A., Maher, K., 2019. Ten-million years of activity within the Eastern California Shear Zone from U–Pb dating of fault-zone opal. Earth Planet. Sci. Lett. 521, 37–45.

Pearthree, P.A., 1993. Geologic and geomorphic setting of the Verde River from Sullivan Lake to Horseshoe Reservoir. Arizona Geological Survey Open File Report 93-4, 1–27.

Pearthree, P.A., House, P.K., 2014. Paleogeomorphology and evolution of the early Colorado River inferred from relationships in Mohave and Cottonwood valleys, Arizona, California, and Nevada. Geosphere 10, 1139–1160.

Pearthree, P.A., Scarborough, R.B., 1985. Reconnaissance analysis of possible Quaternary faulting in central Arizona. Arizona Geological Survey Open File Report, OFR-85-04 (1 map sheet, map scale 1:250,000, 75 p).

Péwé, T.L., 1978. Guidebook to the Geology of Central Arizona. Arizona Bureau of Geology and Mineral Technology Special Paper 2.

Pope, C.W., 1974. Geology of the lower Verde river valley, Maricopa County, Arizona. M.S. thesis. pp. 1–104.

Potochnik, A.R., 1989. Depositional style and tectonic implications of the Mogollon Rim Formation (Eocene), east-central Arizona. In: Anderson, O.J., Lucas, S.G., Love, D.W., Cather, S.M. (Eds.), New Mexico Geological Society Guidebook, 40th Field Conference, Southeastern Colorado Plateau. New Mexico Geological Society, Albuquerque, pp. 107–118.

Powicki, D.A., 1996. The Structural and Metamorphic Geology of the Four Peaks Area, Southern Mazatzal Mountains, Central Arizona. (M.S. thesis). University of Massachusetts, Amherst, Massachusetts.

Reheis, M.C., Edwine, J.L., 2008. Lake Manix shorelines and Afton Canyon terraces: implications for incision of Afton Canyon. Geol. Soc. Am. Spec. Pap. 439, 227–259.

Reheis, M.C., Miller, D.M., Redwine, J.L., 2007. Quaternary stratigraphy, drainage-basin development, and geomorphology of the Lake Manix Basin, Mojave Desert. Guidebook for Fall Field Trip, Friends of the Pleistocene, Pacific Cell, October 4–7, 2007. U.S. Geological Survey Open File Report 2007-1281, 1–31.

Ren, J., Zhang, S., Meigs, A.J., Yeats, R.S., Ding, R., Shen, X., 2014. Tectonic controls for transverse drainage and timing of the Xin-Ding paleolake breach in the upper reach of the Hutuo River, north China. Geomorphology 206, 452–467.

Repasch, M., Karlstrom, K., Heizler, M., Pecha, M., 2017. Birth and evolution of the Rio Grande fluvial system in the past 8 Ma: progressive downward integration and the influence of tectonics, volcanism, and climate. Earth Sci. Rev. 168, 113–164.

Reynolds, S.J., 1985. Geology of the South Mountains, central Arizona. Arizona Bureau of Geology and Mineral Technology Bulletin 195, 1–61.

Reynolds, S.J., Bartlett, R.D., 2002. Subsurface geology of the easternmost Phoenix basin, Arizona: Implications for groundwater flow. Arizona Geological Survey Contributed Report CR-02-A, 1–75.

Reynolds, S.J., Lister, G.S., 1990. Folding of mylonitic zones in Cordilleran metamorphic core complexes: evidence from near the mylonitic front. Geology 18, 216–219.

Richard, S.M., Reynolds, S.J., Spencer, J.E., Pearthree, P.A., 2002. Digital Graphics Files for the Geologic Map of Arizona, A Representation of Arizona Geological Survey Map 35.

Roskowski, J.A., Patchett, P.J., Spencer, J.E., Pearthree, P.A., Dettman, D.L., Faulds, J.E., Reynolds, A.C., 2010. A late Miocene–early Pliocene chain of lakes fed by the Colorado River: evidence from Sr, C, and O isotopes of the Bouse Formation and related units between Grand Canyon and the Gulf of California. Geol. Soc. Am. Bull. 122, 1625–1636.

Savage, J.C., Lisowski, M., Prescott, W.H., 1990. An apparent shear zone trending north-northwest across the Mojave Desert into Owens Valley, eastern California. Geophys. Res. Lett. 17, 2113–2116.

Scarborough, R.B., 1981. Reconnaissance Geology, Salt River from Roosevelt Dam to Granite Reef Dam, central Arizona. Arizona Geological Survey, Open-File Report 81-30 (9 sheets).

Scarborough, R.B., 1989. Cenozoic erosion and sedimentation in Arizona. Arizona Geological Society Digest 17, 515–537.

Seong, Y.B., Dorn, R.I., Yu, B.Y., 2016. Evaluating the life expectancy of a desert pavement. Earth Sci. Rev. 162, 129–154.

Seong, Y.B., Larson, P.H., Dorn, R.I., Yu, B.Y., 2016b. Evaluating process domains in small granitic watersheds: Case study of Pima Wash, South Mountains, Sonoran Desert, USA. Geomorphology 255, 108–124.

Skotnicki, S.J., 1996. Geologic Map of the Bartlett Dam Quadrangle and southern part of the Horseshoe Dam Quadrangle, Maricopa County, Arizona. Arizona Geological Survey Open File Report 96-22, 1–22.

Skotnicki, S.J., 2000. Geologic Map of the Four Peaks 7.5′ Quadrangle, Maricopa and Gila Counties, Arizona. Arizona Geological Survey Open-File Report OFR-00-11 (1 map sheet, map scale 1:24,000, 001–035).

Skotnicki, S.J., 2003. Preliminary geologic map of the Meddler Wash 7.5′ Quadrangle, Gila County, Arizona. Arizona Geological Survey Open File Report OFR-03-04 (1 map sheet, map scale 1:24,000).

Skotnicki, S.J., DePonty, J., 2020. Subsurface Evidence for the Initial Integration of the Salt River, Arizona, Using Clast Assemables of Subsurface Drill Cuttings (Geomorphology this special issue).

Skotnicki, S.J., Ferguson, C.A., 1995. Geological map of the Goldfield quadrangle and the northern part of the Superstition Mountains SW quadrangles, Maricopa and Pinal Counties, Arizona. Arizona Geological Survey Open File Report 95-9, 1–26.

Skotnicki, S.J., Leighty, R.S., 1997. Geological map of the Stewart Mountain Quadrangle, Maricopa County, Arizona. Arizona Geological Survey Open File Report OFR-97-12 (1 map sheet, map scale 1:24,000, 001-019).

Skotnicki, J.S., Leighty, R.S., 1998. Geologic Map of the Boulder Mountain 7.5′ Quadrangle, Maricopa and Gila Counties, Arizona. Arizona Geological Survey Open File Report OFR-98-15 (1 map sheet, map scale 1:24,000, 001-017).

Spencer, J.E., 2011a. 4.8 Ma Age for Inception of the Modern Colorado River Arizona Geology Magazone 12. http://azgeology.azgs.arizona.edu/article/feature-article/2011/2012/2048-ma-age-inception-modern-colorado-river.

Spencer, J.E., 2011b. Preliminary evaluation of Cenozoic basins in Arizona for CO2 sequestration potential. Arizona Geological Survey Open File Report 11-05, 1–14.

Spencer, J.E., Pearthree, P.A., 2001. Headward erosion versus closed basin spillover as alternative causes of neogene capture of the Ancestral Colorado River by the Gulf of California. In: Young, R.A., Spamer, E.E. (Eds.), Colorado River Origin and Evolution: Grand Canyon. Grand Canyon Association, Grand Canyon, pp. 215–219.

Spencer, J.E., Reynolds, S.J., 1989. Middle Tertiary tectonics of Arizona and adjacent areas. Arizona Geological Society Digest 17, 539–574.
Spencer, J.E., Richard, S.M., 1999. Geologic map and report for the Theodore Roosevelt Dam area, Gila and Maricopa Counties, Arizona. Arizona Geological Survey Open File Report 99-6, 1–30.
Spencer, J.E., Richard, S.M., Ferguson, C.A., 2001. Cenozoic structure and evolution of the boundary between the Basin and Range and Transition Zone provinces in Arizona. In: Erskine, M.C., Faulds, J.E., Bartley, J.M., Rowley, P.D. (Eds.), The Geologic Transition, High Plateaus to Great Basin - A Symposium and Field Guide (The Mackin Volume). Utah Geological Association, Salt Lake City, pp. 273–289.
Spencer, J.E., Patchett, P.J., Pearthree, P.A., House, P.K., Sarna-Wojcicki, A.M., Wan, E., Roskowski, J.A., Faulds, J.E., 2013. Review and analysis of the age and origin of the Pliocene Bouse Formation, lower Colorado River Valley, southwestern USA. Geosphere 9. https://doi.org/10.1130/GES00896.00891.
Stewart, J.H., Gehrels, G.E., Barth, A.P., Link, P.K., 2001. Detrital zircon provenance of Mesoproterozoic to Cambrian arenites in the western United States and Northwestern Mexico. Geol. Soc. Am. Bull. 113, 1343–1356.
Stone, J., 1998. A rapid fusion method for separation of Beryllium-10 from soils and silicates. Geochim. Cosmochim. Acta 62, 555–561.
Valletta, R.D., Willenbring, J.K., Lewis, A.R., Ashworth, A.C., Caffee, M., 2015. Extreme decay of meteoric beryllium-10 as a proxy for persistent aridity. Sci. Rep. 5, 17813. https://doi.org/10.1038/srep17813.
von Blanckenburg, F., Bouchez, J., Wittmann, H., 2012. Earth surface erosion and weathering from the 10Be (meteoric)/9Be ratio. Earth Planet. Sci. Lett. 351–352, 295–305.
Willenbring, J.K., von Blanckenburg, F., 2010. Meteoric cosmogenic Beryllium-10 adsorbed to river sediment and soil: applications for Earth-surface dynamics. Earth-Sci. Rev. 98, 105–122.
Withjack, M.O., Schlische, R.W., Olsen, P.E., 2002. Rift-basin structure and its influence on sedimentary systems. SEPM Spec. Publ. 73, 58–81.
Youberg, A., Pearthree, P.A., Cook, J.P., Gootee, B.F., Douglass, J.D., Heizler, 2020. Development and integration of the middle Gila River in the Safford basin, southeast Arizona. Geomorphology 369 (in press).